Naturalis Biodiversity Center

Naturalis Repository

Climatic oscillations, dispersibility and adaptability behind worldwide mountain radiations of the Helichrysum–Anaphalis–Pseudognaphalium (HAP) clade (Compositae)

Carme Blanco-Gavaldà, Renske E. Onstein, Luís Valente [and others]

Downloaded from:
https://doi.org/10.1093/aob/mcaf110

Article 25fa Dutch Copyright Act (DCA) - End User Rights
This publication is distributed under the terms of Article 25fa of the Dutch Copyright Act (Auteurswet) with consent from the author. Dutch law entitles the maker of a short scientific work funded either wholly or partially by Dutch public funds to make that work publicly available following a reasonable period after the work was first published, provided that reference is made to the source of the first publication of the work.

This publication is distributed under the Naturalis Biodiversity Center 'Taverne implementation' programme. In this programme, research output of Naturalis researchers and collection managers that complies with the legal requirements of Article 25fa of the Dutch Copyright Act is distributed online and free of barriers in the Naturalis institutional repository. Research output is distributed six months after its first online publication in the original published version and with proper attribution to the source of the original publication.

You are permitted to download and use the publication for personal purposes. All rights remain with the author(s) and copyrights owner(s) of this work. Any use of the publication other than authorized under this license or copyright law is prohibited.

If you believe that digital publication of certain material infringes any of your rights or (privacy) interests, please let the department of Collection Information know, stating your reasons. In case of a legitimate complaint, Collection Information will make the material inaccessible. Please contact us through email: collectie.informatie@naturalis.nl. We will contact you as soon as possible.

Annals of Botany **00**: 1–22, 2025
https://doi.org/10.1093/aob/mcaf110, available online at www.academic.oup.com/aob

ANNALS OF BOTANY
Founded 1887

ORIGINAL ARTICLE

Climatic oscillations, dispersibility and adaptability behind worldwide mountain radiations of the *Helichrysum–Anaphalis–Pseudognaphalium* (HAP) clade (Compositae)

Carme Blanco-Gavaldà[1,*], Renske E. Onstein[2,3], Luís Valente[2,4], Thijs Janzen[4], Santiago Andrés-Sánchez[5], Nicola Bergh[6,7], Juan Antonio Calleja[8], Pau Carnicero[1,9], Òscar Castillo[1], Glynis V. Cron[10], Frederik Leliaert[11], Lucía D. Moreyra[12], Genís Puig-Surroca[12], Sylvain G. Razafimandimbison[13], Alfonso Susanna[12], Cristina Roquet[12,†] and Mercè Galbany-Casals[1,†]

[1]Systematics and Evolution of Vascular Plants (UAB) – Associated Unit to CSIC by IBB, Department of Animal Biology, Plant Biology and Ecology, Autonomous University of Barcelona, ES-08193 Bellaterra, Spain, [2]Naturalis Biodiversity Center, 2333 CR Leiden, The Netherlands, [3]German Centre for Integrative Biodiversity Research (iDiv) Halle–Jena–Leipzig, 04103 Leipzig, Germany, [4]Groningen Institute for Evolutionary Life Sciences, University of Groningen, 9700 CC Groningen, The Netherlands, [5]Department of Botany and Plant Physiology and Plant DNA Biobank, University of Salamanca, ES-37007 Salamanca, Spain, [6]Gothenburg Botanical Garden, 413 19 Gothenburg, Sweden, [7]South African National Biodiversity Institute, 7735 Cape Town, South Africa, [8]Department of Botany, Autonomous University of Madrid, 28049 Madrid, Spain, [9]Department of Botany, University of Innsbruck, 6020 Innsbruck, Austria, [10]School of Animal, Plant & Environmental Sciences, University of Witwatersrand, 2050 Johannesburg, South Africa, [11]Meise Botanic Garden, BE-1860 Meise, Belgium, [12]Botanic Institute of Barcelona (IBB, CSIC – Ajuntament de Barcelona), ES-08038 Barcelona, Spain, and [13]Swedish Museum of Natural History, SE-104 05 Stockholm, Sweden
[*]For correspondence. E-mail carme.blanco@uab.cat
[†]Co-senior authors.

Received: 26 February 2025 Returned for revision: 24 April 2025 Editorial decision: 29 May 2025 Accepted: 29 May 2025

• **Background and Aims** Mountain ecosystems are recognized as biodiversity hotspots. However, the origins of their remarkable diversity remain unresolved. We explore this question by focusing on the HAP clade (*Helichrysum–Anaphalis–Pseudognaphalium*), a megadiverse lineage within the family Compositae that spans tropical and temperate mountain and lowland systems worldwide. The existence of multiple high-elevation clades provides an opportunity to address hypotheses regarding the impact of trait innovation, climatic oscillations, dispersal and niche lability in the diversification of mountain lineages.
• **Methods** To investigate the biogeographical history and diversification dynamics of the HAP clade, we built a time-calibrated phylogeny of 560 taxa (62 % of the species) based on 989 nuclear loci. We examined the frequency of inter-mountain dispersal and lowland-to-mountain transitions and vice versa, tested whether diversification rates were dependent on time, climate or species diversity, and assessed the impact of bract colour on diversification rates using state-dependent speciation–extinction models. Additionally, we reconstructed the evolutionary history of two functional traits (bract colour, life form) and ecological preferences (elevational range, habitat) and explored potential correlations between them.
• **Key Results** The HAP clade extensively speciated during the Pleistocene, when net diversification rates nearly quadrupled, coinciding with parallel mountain radiations on multiple continents. The clade followed a pattern of nested radiations, with southern African mountains serving as the initial diversity source and other mountain systems acting primarily as sinks. High-elevation ecosystems also contributed to lowland biodiversity. Diversification rates in high elevations are independent of bract colour, yet significant trait–environment associations were supported. Functional traits and ecological preferences evolved repeatedly, with a tendency toward montane open habitat ecologies and chamaephytic life forms.
• **Conclusions** Our findings suggest that mountains do not fit the classic island model for the HAP clade due to its high permeability across heterogeneous environments, high dispersibility, and ability to thrive in both high and low elevations. However, the clade's evolutionary lability enabled repeated trait acquisition, niche shifts and microhabitat specialization. This, coupled with Pleistocene climatic instability, probably played a significant role in driving allopatric and ecological speciation at different geographical scales.

© The Author(s) 2025. Published by Oxford University Press on behalf of the Annals of Botany Company. All rights reserved. For commercial re-use, please contact reprints@oup.com for reprints and translation rights for reprints. All other permissions can be obtained through our RightsLink service via the Permissions link on the article page on our site—for further information please contact journals.permissions@oup.com.

Key words: *Helichrysum*, HAP clade, *Anaphalis*, *Pseudognaphalium*, *Achyrocline*, diversification, high elevation, Pleistocene, radiations, specialization, adaptability, long-distance dispersal.

INTRODUCTION

Mountain ecosystems worldwide are recognized as biodiversity hotspots, hosting disproportionately high levels of plant endemics relative to their small size (Antonelli, 2015; Hughes and Atchison, 2015; Merckx *et al*., 2015) and contributing significantly to the global angiosperm richness. These ecosystems are often recognized as natural laboratories, offering great spatial and climatic heterogeneity and housing pronounced environmental gradients over short distances (Körner *et al*., 2011). Understanding the primary drivers of mountain biodiversity and diversity turnover is crucial for unravelling its origins and developing data-driven strategies for ensuring its future maintenance. Current research suggests that exceptional mountain diversity results from the combination of abiotic and biotic factors, whose additive interactions create unique conditions that promote speciation and species persistence over time (Nürk *et al*., 2020).

The main abiotic drivers of diversification in mountain ecosystems are associated with geological and climatic variation at small scales, including factors such as elevation, slope, soil (Antonelli *et al*., 2018; Perrigo *et al*., 2020), temperature and precipitation (Muellner-Riehl *et al*., 2019). Deep-time historical processes, such as orogeny and climatic oscillations that transformed previously mature landscapes, are also crucial to explain current biodiversity. Some studies indicate that net diversification rates declined during the Pleistocene due to climatic instability, extinction and range contractions, particularly in lineages with low dispersal ability or high specialization (Sandel *et al*., 2017). However, substantial evidence supports the idea that Pleistocene climate oscillations had positive effects on diversification rates in both tropical (e.g. *Hypericum* L., Nürk *et al*., 2015) and temperate (e.g. bamboos, Ye *et al*., 2019; *Jurinea* Cass., Herrando-Moraira *et al*., 2023) mountain radiations, creating new opportunities and barriers that led to repeated cycles of migration and isolation, acting as a 'species pump' (Flantua and Hooghiemstra, 2018). Many plant radiations (understood as episodes of rapid diversification, resulting in high species richness, Hughes and Eastwood, 2006) coincided with Pleistocene climate variations, while only a few pre-dated the Mid-Miocene Climate Optimum (around 15–18 Ma, Böhme, 2003), none of them in temperate areas (Muellner-Riehl *et al*., 2019). Similarly, rapid mountain uplift has been associated with increased diversification rates (e.g. Andean Páramos, Madriñán *et al*., 2013). An additional mechanism to explain high mountain diversity is long-distance dispersal, which seems to have played a key role in providing preadapted lineages from geographically distant regions (Edwards and Donoghue, 2013) as observed in various mountain systems (e.g. Malaysia, Merckx *et al*., 2015; Afroalpine region, Kandziora *et al*., 2022). Tropical mountains are renowned for this, for which strong phylogenetic evidence suggests that both tropical and, more predominantly, distant temperate regions have served as important sources of their diversity (Galley and Linder, 2006; Gehrke and Linder, 2009; Sklenář *et al*., 2011; Nürk *et al*., 2018; Blanco-Gavaldà *et al*., 2023, 2025).

Among biotic drivers of diversification, key innovations (i.e. newly evolved traits that enable organisms to exploit previously inaccessible niches) are the most relevant (Miller *et al*., 2023). Although few studies have quantified the impact of key innovations on diversification rates in mountain plants (e.g. Merianieae, Dellinger *et al*., 2024; *Juniperus* L., Liu *et al*., 2024), the acquisition of specific traits seems crucial to face the extreme environmental conditions of high-elevation habitats, such as high UV radiation and freezing temperatures or low pollinator availability. The most studied innovations are related to life forms and include the acquisition of perenniality (*Lupinus* L. in the Andes, Drummond *et al*., 2012), cushion growth (*Androsace* L. in Eurasia, Roquet *et al*., 2013) and woodiness (in Afroalpine *Alchemilla* L., Gehrke *et al*., 2016). In tropical mountains, gigantism [e.g. *Lobelia* Mill. and *Dendrosenecio* (Hauman ex Hedberg) B.Nord in eastern tropical Africa mountains, *Espeletia* Mutis ex Bonpl. and *Puya* Molina in the Andes] provides adaptive advantages against abiotic stressors such as freezing and water scarcity (Brochmann *et al*., 2022 and references therein). These species are often associated with damp microenvironments such as stream borders and gullies (Hedberg, 1964). In contrast, temperate mountain species tend to develop compact cushion-like forms that protect persistent buds near the ground, offering greater resistance to cold and wind exposure (Hedberg, 1964; Nürk *et al*., 2019; Körner, 2021). Furthermore, certain floral traits, such as large white flowers, may have evolved not only to attract generalist pollinators present at high elevations (Diptera and Coleoptera) but also to reflect UV radiation (Hedberg, 1964; Lefebvre *et al*., 2018; Baumann *et al*., 2021; Körner, 2021) and even to enable nyctinastic movements to protect the reproductive organs during the night (Minorsky, 2019). Nevertheless, trait flexibility and lineage adaptability might exert a stronger influence on diversification rates than any single innovation (Onstein, 2020; Helmstetter *et al*., 2023).

Some plant groups have diversified more extensively than others in mountain systems, though the reasons for this disparity remain poorly understood. To date, diversification dynamics have been studied for a few species-rich mountain lineages, such as *Lupinus* (Drummond *et al*., 2012; Contreras-Ortiz *et al*., 2018), *Jurinea* (Herrando-Moraira *et al*., 2023) and Ericaceae (Schwery *et al*., 2015; Pirie *et al*., 2019). Moreover, recent studies suggest that diversification rates and species richness in plants are independent, with greater species richness in humid tropical areas and higher diversification rates in heterogeneous environments with high species turnover (Kandziora *et al*., 2022; Tietje *et al*., 2022; Tenorio *et al*., 2023). This underscores the need for further research on the biogeographical history and diversification drivers of other highly diversified plant clades, particularly those spanning both temperate and tropical mountains. It would also be important to include key biodiversity hotspots, such as Madagascar and the southern African region, whose mountains remain understudied from an evolutionary perspective (Rudbeck *et al*., 2022).

In this context, we focus on the HAP clade (comprising *Helichrysum* Mill., *Anaphalis* DC., *Pseudognaphalium* Kirp. and several smaller genera; Smissen *et al*., 2011; Galbany-Casals *et al*., 2014; Nie *et al*., 2016), which comprises a total of *c*. 800

species (Hilliard, 1983; Anderberg, 1991), as a relevant study-case. This clade belongs to the Compositae, the most diverse plant family in high-elevation environments such as the Andes (Pérez-Escobar *et al.*, 2022), the Afroalpine area (Gehrke and Linder, 2014), the Asian mountains (Yu *et al.*, 2020) and the southern African Drakensberg (Carbutt and Edwards, 2004; Carbutt, 2019). The HAP clade is particularly suited for studying mountain plant diversification due to its wide geographical distribution across tropical and temperate mountain systems and its richness in widespread and also narrowly endemic species. *Helichrysum* is the largest genus in the HAP clade, particularly diverse in southern Africa (*c.* 250 species, over half of which are in mountain habitats; Hilliard, 1983), the tropical Afromontane and Afroalpine regions (*c.* 72 species; Lisowski, 1989; Beentje, 2002; Tadesse, 2004) and Madagascar (111 species, half of them montane; Humbert, 1962), although it is also present in the Mediterranean Basin and Macaronesia. *Anaphalis* (110 species; Anderberg, 1991) and *Pseudognaphalium* (90 species; Anderberg, 1991) predominate in the mountains of Asia and the Americas, respectively. This distribution pattern suggests multiple independent mountain radiations, but this has yet to be confirmed because a solid and comprehensive phylogenetic framework is lacking for this megadiverse pan-montane group. The HAP clade shows remarkable adaptability, with species growing in a wide range of climatic conditions, thriving in diverse biomes, ranging from montane grasslands and alpine culminal rocky areas to coastal dunes and semideserts. While shrubby forms dominate, the clade displays a wide range of growth forms, from annual herbs to small trees, and there is a high diversity in reproductive strategies reflected in the varied number, size and disposition of capitula, the number of florets, and the colour and size of the involucral bracts (Anderberg, 1991). We observed that high-elevation species tend to have white involucral bracts, a trait that could have enhanced diversification in those environments. Additionally, we also noted that specific life forms seem to be associated with certain habitats across the clade's geographical range.

This study aims to advance our understanding of plant diversification in high-elevation environments by applying an integrative approach. Combining data from multiple sources we investigate the biogeographical and diversification dynamics of the HAP clade and the roles of trait evolution and Pleistocene climatic oscillations in its evolutionary history. Based on previous works for tropical African and Malagasy mountain lineages (Blanco-Gavaldà *et al.*, 2023, 2025), we hypothesize that: (H1) diversification in the HAP clade fits a pattern of nested radiations in mountain systems worldwide, in which southern African mountains act as the main source and other mountain regions serve as a sink, with occasional cross-seeding events (Linder, 2014; Linder and Verboom, 2015); (H2) the current biodiversity distribution patterns of the HAP clade result from the combination of long-distance dispersals of preadapted ancestors from distant regions with similar biomes (in line with the niche conservatism principle; Wiens *et al.*, 2010) alongside *in situ* diversification due to habitat specialization in regions with high environmental heterogeneity (Rundell and Price, 2009; Edwards and Donoghue, 2013) and regional allopatric speciation; (H3) in high-elevation HAP clade lineages, Pleistocene climatic oscillations had a greater impact on diversification rates than the acquisition of key functional traits that are nowadays common in high-elevation species; and (H4) convergent adaptation to particular microhabitats shaped trait–environment associations in mountain systems, since certain functional traits are repeatedly shared among species inhabiting specific habitats, suggesting convergent adaptation to similar environments. To test these hypotheses, we built the most comprehensive time-calibrated phylogeny of the HAP clade to date, using a family-specific target-enrichment probe set and building on a wide taxonomic sampling that includes 62 % of the species and a balanced representation of the morphological and ecological variation of the study group throughout the globe and elevational belts. We inferred the clade's ancestral biogeographical ranges to assess its area of origin, its propensity for long-distance dispersal, and the contribution of elevational and latitudinal transitions to mountain biodiversity. We also assessed the evolution and ancestral states of key functional traits frequent in high-elevation species (i.e. having whitish bracts and being a cushion-like or gigantic shrubs, depending on the latitude) and ecological preferences. Finally, we evaluated macroevolutionary dynamics by testing whether diversification rates varied with time, climate, species diversity, or the acquisition of specific traits and whether functional traits (bract colour and life form) are correlated with certain ecological variables (elevation and habitat preferences).

MATERIALS AND METHODS

Taxon sampling and laboratory workflow

To reconstruct the evolutionary history of the HAP clade, we used sequences from 526 samples (including 500 species and 24 infraspecific taxa), which represent *c.* 62 % of the clade's diversity (*c.* 800 species in total) and cover all major clades, genera and morphological variations (Supplementary Data Table S1), as well as all distribution areas (Table S2), and ecological and elevational preferences (Table S3). The largest genus, *Helichrysum*, is represented by 400 samples (393 species, 73 % of species). All the smaller genera known to be nested within *Helichrysum* are also included (Smissen *et al.*, 2011; Galbany-Casals *et al.*, 2014; Nie *et al.*, 2016): *Achyrocline* Less. (15 species, 47 %), *Anaphalis* (39 species, 37 %), *Galeomma* Rauschert (one species, 50 %), *Humeocline* Anderb. (one species, 100 %), *Pseudognaphalium* (62 species, 69 %), *Stenocline* DC. (two species, 100 %), *Stenophalium* Anderb. (two species, 40 %) and *Syncephalum* DC. (one species, 20 %).

Based on previous phylogenetic works (Nie *et al.*, 2016; Smissen *et al.*, 2020), we added 34 additional species from the Gnaphalieae to allow calibration for divergence time estimation, resulting in a dataset of 560 samples (Supplementary Data Table S1). A total of 124 samples corresponding to 121 species were newly sequenced. The other 436 samples, corresponding to 418 species, were taken from prior studies (329 samples from Blanco-Gavaldà *et al.*, 2023, BioProject PRJNA936872; 91 from Blanco-Gavaldà *et al.*, 2025, BioProject PRJNA1121119; six from Mandel *et al.*, 2019, BioProject PRJNAS40287; and ten from Schmidt-Lebuhn and Bovill, 2021, BioProject PRJNA665592). We targeted the set of genomic loci included in the Compositae COS 1061 loci kit (Mandel *et al.*, 2014), which was specifically designed for this plant family. We followed the target-enrichment library preparation and sequence capture protocols described in Blanco-Gavaldà *et al.* (2023). The newly generated DNA sequence reads have been deposited in the NCBI Sequence Read Archive database (SRA; access: https://www.ncbi.nlm.nih.gov/sra) under the BioProject

accession number PRJNA1219322 (see unique sample accession numbers in Table S1).

Molecular data processing and phylogenetic analyses

We adhered to the workflow outlined in Blanco-Gavaldà *et al.* (2023) based on the use of HybPhyloMaker (Fér and Schmickl, 2018, available at https://github.com/tomas-fer/HybPhyloMaker, hereafter referred to as HPM, along with the corresponding script number) in conjunction with ParalogWizard (Ufimov *et al.*, 2022, available at https://github.com/rufimov/ParalogWizard), to extract the targeted 1061 COS loci and detect and separate paralogues before generating orthologous alignments.

Trimmomatic v.0.39 (Bolger *et al.*, 2014) was used to eliminate adaptors and low-quality reads and BBMap v.38.42 (Bushnell, 2014) was used to remove duplicate sequences (HPM1). BWA (Li and Durbin, 2009) and SPAdes (Bankevich *et al.*, 2012) were used to create an initial reference file for read mapping based on *Helianthus annuus* L. genome sequences from the Compositae1061 probe set (Mandel *et al.*, 2014). Subsequently, we generated a customized reference using our ingroup samples to enhance mapping specificity. ParalogWizard was used to identify potential paralogues based on a pairwise exonic sequence divergence calculation, which generated a histogram with two distinct peaks: the first representing putative allelic variation and the second indicating highly divergent sequences that are probably paralogues (Supplementary Data Fig. S1). We used the peak range values as a threshold to extract putative paralogous sequences. Finally, we used MAFFT v.7.475 (Katoh and Toh, 2008) to align sequences in orthologous matrices and to concatenate exons into putative loci. To minimize missing data, we excluded sequences with over 70 % of missing data and removed loci that were present in fewer than 75 % of all samples (HPM5).

Phylogenetic analyses were based on both concatenation and coalescence-based methods. For the first approach, we combined all nuclear loci to generate a supermatrix and estimated the optimal nucleotide substitution model for each locus using ModelTest-NG (Darriba *et al.*, 2020). This was followed by maximum likelihood (ML) partitioned analyses in which we used RAxML-NG v.1.1.0 (Kozlov *et al.*, 2019) to run 20 independent ML tree searches (modified HPM8f), branch support being assessed via bootstrap (inference set to automatically determine a sufficient number of bootstrap replicates). The highest-scoring ML tree was annotated with Felsenstein's bootstrap (BS; Felsenstein, 1985) and transfer bootstrap expectation (TBE; Lemoine *et al.*, 2018) values, where branches with BS $\geq$ 70 % and TBE $\geq$ 0.7 were regarded as statistically supported (Hillis and Bull, 1993; Lemoine *et al.*, 2018). For the coalescent-based approach, we performed summary-coalescence inference with ASTRAL-III v.5.7.8 (Zhang *et al.*, 2018) based on individual gene trees for each locus inferred with RAxML v.8.2.12 (Stamatakis, 2014; HPM6a, HPM7 and HPM8a). Branch support was assessed via local posterior probability (LPP) values, with branches considered well-supported if they had LPP $\geq$ 0.95 (Sayyari and Mirarab, 2016). In all cases, trees were rooted using Newick utilities (Junier and Zdobnov, 2010) on four outgroup species representing four genera of the subtribe Relhaniinae, which is known to be the sister clade to the subtribe Gnaphaliinae (Bayer *et al.*, 2000; Bergh and Linder, 2009; Montes-Moreno *et al.*, 2010; Smissen *et al.*, 2020): *Athrixia phylicoides* DC., *Leysera gnaphalodes* Thunb., *Phagnalon sordidum* (L.) Rchb. and *Oedera pungens* (L'Hér.) N.G.Bergh.

Divergence time estimation

We used RelTime (Tamura *et al.*, 2012, 2018) available in the software MEGA X (Kumar *et al.*, 2018) to estimate divergence times by relaxing the strict molecular clock assumption on the ML phylogeny that yielded the highest likelihood with the concatenation approach. We based our analyses on the ML tree because branch length estimates from concatenation-based analyses are generally more accurate than those from coalescent-based approaches, which tend to underestimate evolutionary change (Schwartz and Mueller, 2010). Confidence intervals were calculated using the method of Tao *et al.* (2020), also implemented in RelTime. This dating method is effective for large empirical genomic datasets and accommodates the use of calibration densities (Costa *et al.*, 2022). The Gnaphalieae tribe lacks sufficient ancient fossils to serve as primary calibration points. To incorporate fossil calibration points, we would need to sample other Compositae tribes, which was beyond the scope of our study. Thus, we employed five secondary calibration points (CPs; indicated on the tree in Supplementary Data Fig. S2) derived from previously estimated divergence times by Nie *et al.* (2016), who employed Bayesian inference methods to estimate divergence times using a relaxed clock model for the Gnaphalieae tribe. We acknowledge the potential limitations of relying on secondary calibration points derived from a single study; however, we chose to do so because the other few studies that estimated divergence times within the Gnaphalieae have a more limited sample size than the work of Nie *et al.* (2016), and limited sampling is known to strongly affect dating estimations (Linder *et al.*, 2005). We also included a fifth calibration point, based on geological evidence, specifically the emergence of Madeira (Ramalho *et al.*, 2015). We utilized a normal density distribution for the secondary calibration points, which yielded mean and standard deviation values that reflect the 95 % confidence interval outlined in the original study: the tribe crown node with a mean age of 25 Ma and a standard deviation of ±2.55 (CP1), the 'crown radiation' node with a mean age of 20.7 Ma and a standard deviation of ±2.55 (CP2), the 'HAP clade' crown node with a mean age of 15.39 Ma and a standard deviation of ±1.95 (CP3), the 'FLAG clade' crown node with a mean age of 12.78 Ma and a standard deviation of ±1.85 (CP4) and the '*Anaphalis* + Mediterranean–Asian *Helichrysum*' crown node with a mean age of 7.04 Ma and a standard deviation of ±0.85 (CP5). Additionally, the emergence of Madeira at 5.6 Ma (CP6) was set as a maximum age constraint for the stem node of the lineage that includes the four endemic *Helichrysum* species from the archipelago (Galbany-Casals *et al.*, 2014). Future studies may benefit from the incorporation of fossil calibrations to further refine divergence time estimates; however, this would require expanding the sampling with representatives of several Compositae tribes and appropriate outgroup taxa.

Ancestral biogeographical range inference

Taking into account the general distribution patterns of the HAP clade, we defined six large areas and subdivided them

into two elevational belts (lowlands vs. mountains) resulting in 12 regions (species coded in Supplementary Data Table S2): (A) Southern Africa lowlands, (B) Southern Africa mountains, (C) Tropical Africa lowlands, (D) Tropical Africa mountains, (E) Madagascar lowlands, (F) Madagascar mountains, (G) Eurasia lowlands, (H) Eurasia mountains, (I) North and Central America lowlands, (J) North and Central America mountains, (K) South America lowlands and (L) South America mountains. Recognizing that elevational belts depend heavily on latitude and environmental factors such as precipitation, orientation and continentality, among others (Körner *et al*., 2011; Körner, 2021), we applied a broad and simplified classification to identify general patterns on a global scale. Our classification mainly follows Kandziora *et al*. (2016), which distinguishes tropical and temperate regions to account for the latitudinal effect (i.e. elevational belts are shifted towards lower elevations at higher latitudes). Thus, we categorized species into two elevational stages: (1) lowlands, below 800 m above sea level in temperate latitudes and below 1800 m in tropical latitudes, and excluding those primarily inhabiting mountain massifs; and (2) mountains (including the montane to alpine belts, considered high-elevation species along the study), above 800 m in temperate latitudes and above 1800 m in tropical latitudes – except in Madagascar, where the boundary was adjusted to 1300 m, based on species distribution patterns specific to the microcontinent (Humbert, 1962, as in Blanco-Gavaldà *et al*., 2025). Species were only classified as high-elevation if they primarily inhabited mountains or massifs, rather than highlands, regardless of elevation (Körner *et al*., 2011). By focusing on mountains vs. highlands instead of just elevation, we account for the environmental heterogeneity of mountains and the effects of relief in climatology. Although this approach may overlook how elevation alone, along with associated variables such as temperature, influences species distributions, it aligns better with our primary goal of assessing the role of mountains on broad biogeographical patterns across the entire clade's distribution.

To assign an area to each species, we compiled distribution and elevational data for the HAP clade, documenting the minimum and maximum elevation limits based on reference Floras (Supplementary Data References) and herbarium records from GBIF and institutional collections (mainly from BC, BCN, BNRH, BR, CANB, CONC, E, FM, LP, MA, MADJ, MBK, MEXU, MO, NBG, NY, O, P, PRE, RSA, S, SALA, SI, US and W). For species that occasionally extend beyond their core distribution range, we only considered the area or elevational stage where most occurrences are concentrated, disregarding marginal presences. While we aimed for a threshold of >90 % of occurrences, we often adjusted the classification based on expert knowledge on each species' preferences.

We conducted ancestral biogeographical range inference analyses on the ML time-calibrated phylogeny to identify the origin area of the HAP clade (H1) and to trace the colonization events into high-elevation regions (H2). Using the R package BioGeoBEARS (Matzke, 2013), we limited the maximum number of areas for any given node to three, reflecting the highest number of areas occupied by the most widely distributed extant taxon in this work. We compared the fit of six biogeographical models: Dispersal–Extinction–Cladogenesis (DEC; Ree *et al*., 2005; Ree and Smith, 2008), a likelihood-based version of the Dispersal–Vicariance model (DIVAlike; Ronquist, 1997) and the BayArea model (BAYAREAlike; Landis *et al*., 2013), along with the respective versions of each model that incorporate founder-event speciation by adding a jump-dispersal parameter (+j). DEC models generally provide a better fit to the data than the DIVA and BayArea models, which are more restrictive (Matzke, 2013). In particular, BayArea assumes that no range evolution occurs at cladogenesis (i.e. the ancestral range is inherited by both daughter lineages, Landis *et al*., 2013). This assumption can be problematic, especially at large geographical scales, as it oversimplifies complex biogeographical processes like range expansion, contraction and the existence of dispersal barriers such as oceans and mountains ranges. In recent years, debate has emerged regarding the incorporation of the founder-event parameter (+j) in event-based biogeographical models. Ree and Sanmartín (2018), on the basis of two small manually created datasets, presented theoretical arguments questioning the validity of statistically comparing DEC and DEC+j models. However, a more comprehensive simulation-based study (Matzke, 2022) proved that log-likelihood comparisons between DEC and DEC+j models are statistically valid. Conceptually, it is reasonable to assume that lineage splitting and jump dispersal events can occur simultaneously, especially over timescales of millions of years. As we discussed in a previous study, where we compared the DEC and DEC+j biogeographical reconstructions (Blanco-Gavaldà *et al*., 2023), the DEC+j model provides more realistic range estimations, particularly suited for widespread and recently diversified lineages, which include many mountain and island endemics.

We selected the optimal model according to the Akaike Information Criterion (AIC; Burnham and Anderson, 1998). We performed Biogeographic Stochastic Mapping (BSM; Dupin *et al*., 2017) using 100 BSM replicates under the best-fitting biogeographical model to assess the role of mountain systems as sources or sinks of biodiversity (H1) across its whole distribution and the frequency of lineage exchanges (H2) between similar biomes (lowland to lowland, mountain to mountain) or biome shifts (lowland-to-mountain and vice versa). BSM analyses provide a probabilistic estimate of the timing, frequency, directionality and types of biogeographical events (anagenetic dispersals, cladogenetic range expansions, founder events and extinctions) between areas. Based on the BSM outputs, we plotted temporal diversity across the biogeographical regions using the R package *ltstR* v.0.1.0 (Skeels, 2019), extracting the number of species present in each region at a time point.

Ancestral state reconstruction of functional and ecological traits

To investigate how functional traits and ecological preferences evolved within the HAP clade (H2), we estimated ancestral states for two functional traits (involucral bract colour and life form) and two ecological preferences (elevational range and habitat preference). We scored 518 ingroup species (see classification in Supplementary Data Table S3) using reference Floras (Supplementary Data References), herbarium specimens, protologues and our field observations. Bract colour was categorized as either: (1) whitish, sometimes with pink-red tints, or (2) yellow-brown (Fig. 1). Elevational range preference followed the criteria outlined in the ancestral biogeographical range inference section, but here additionally splitting mountain species in preference for montane or alpine belts. The alpine belt includes species that predominantly grow above the treeline, generally >2000 m in temperate latitudes and

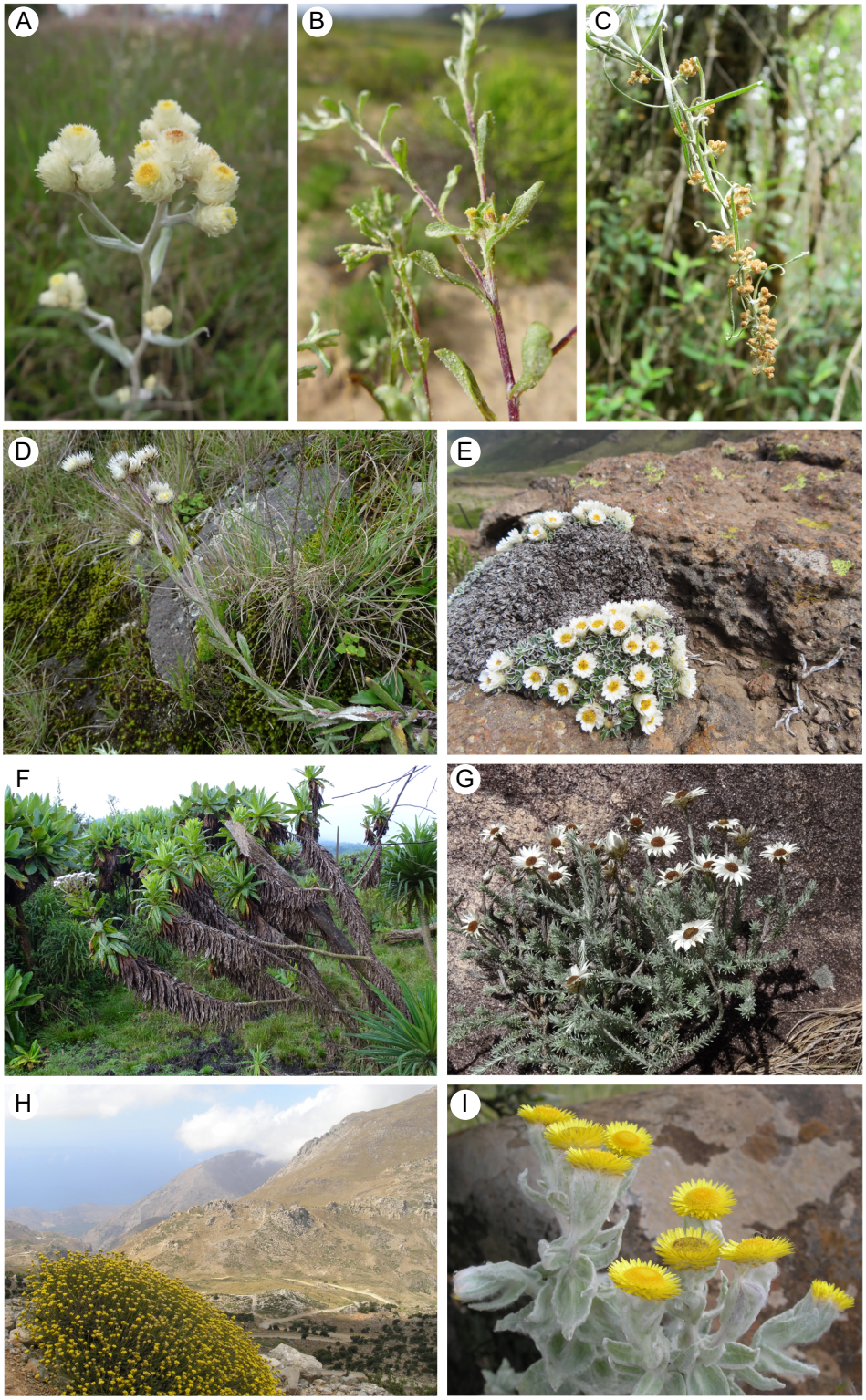

FIG. 1. Specimens illustrating the seven most common life forms within the HAP clade defined in the study along with clear examples of the two most frequent involucral bract colours: (A) *Pseudognaphalium jaliscence* (Greenm.) Anderb. and (B) *Helichrysum micropoides* DC., both therophytes inhabiting open lowland habitats in North America and South Africa, respectively; (C) *Helichrysum mutisiifolium* Less., a lianescent form found in Malagasy montane forests; (D) *H. milbraedii* Moeser, a hemicryptophyte from tropical Africa open montane habitats; (E) *H. sessilioides* Hilliard, a cushion-like chamaephyte growing on Drakensberg rocks, South Africa; (F) *H. formosissium* Sch.Bip., a macrophanerophyte from tropical Africa montane forests; (G) *H. danguyanum* Humbert, a chamaephyte in Malagasy rocky montane habitats, exemplifying white involucral bracts; (H) *H. italicum* subsp. *microphyllum* (Willd.) Nym., a nanophanerophyte from Mediterranean open montane habitats; and (I) *H. albilanatum* Hilliard, a chamaephyte from South African open montane grasslands, illustrating yellow involucral bracts. Photo credits: Mercè Galbany-Casals, except for (B) Santiago Andrés-Sánchez and (E) Deon du Plessis.

>3200 m in tropical latitudes (Körner *et al.*, 2011; Körner, 2021). Life forms were divided into seven states (Fig. 1): (1) therophytes; (2) hemicryptophytes; (3) chamaephytes; (4) cushion-like chamaephytes; (5) nanophanerophytes, with persistent buds between 25 and 150 cm above ground; (6) macrophanerophytes, with persistent buds above 150 cm; and (7) lianescent forms. Species exhibiting plasticity between two states were assigned to the most common or representative category (e.g. some species may behave as therophytes or chamaephytes depending on environmental conditions, while others can be classified either as chamaephytes or nanophanerophytes due to their variability in size). Habitat preference was treated as five discrete states (Fig. 2): (1) permanently humid habitats, such as stream borders, wetlands and deep gullies; (2) open habitats such as shrublands, grasslands and disturbed habitats, including large forest clearings; (3) rocky habitats such as crevices or scree, considering here only strictly rupicolous species; (4) forests, considering here only species growing in the shaded understorey or very small clearings, partly shaded; and (5) deep sands, mainly coastal dunes but also inner deserts.

To infer the evolutionary transitions between different trait states along the phylogeny, we used Markov models (Mk) implemented in the R package *diversitree* (FitzJohn, 2012). For each trait, we fitted and compared three Mk models using AIC values: (1) an all-rates-different model (ARD), (2) a symmetrical model in which the transition rates between any two specific states are equal (SYM) and (3) an equal-rates model, constraining all transitions to a single rate (ER).

Time-, climate- and diversity-dependent macroevolutionary dynamics of the HAP clade

To assess the general drivers of diversification of the HAP clade (H3) we studied its macroevolutionary dynamics, fitting and comparing diversification models based on explicit hypotheses. Utilizing a hypothesis-driven approach is recommended to mitigate identifiability issues (Louca and Pennell, 2020; Morlon *et al.*, 2022). We tested whether the rates of speciation and extinction exhibited a linear or exponential variation in relation to time or environmental changes (specifically global temperature fluctuations based on Zachos *et al.*, 2008) using the R package *RPANDA* (Morlon *et al.*, 2016). We also used the R package *DDD* (Etienne *et al.*, 2012) to test whether speciation was influenced by species diversity, incorporating the carrying capacity (K), which represents the maximum number of species that can coexist, as an additional parameter. Lastly, to determine if there was a notable shift in diversification dynamics throughout the history of the HAP clade, we fitted diversity-dependent models that

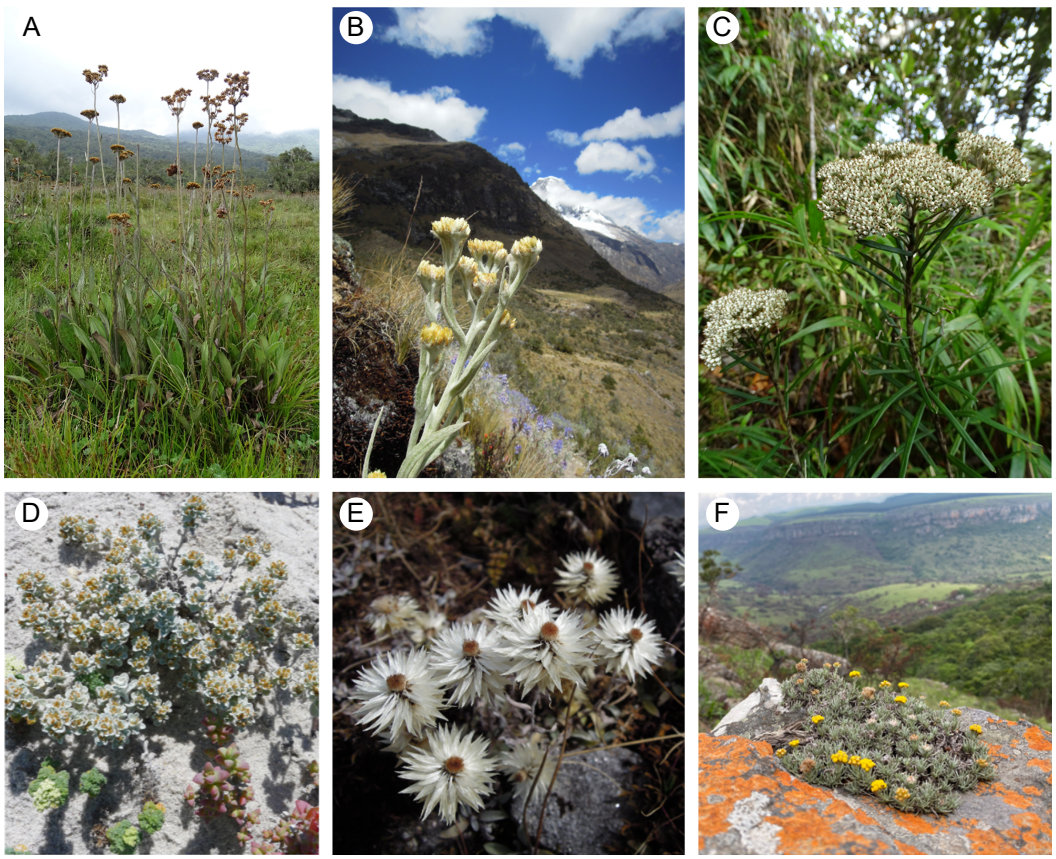

FIG. 2. Representative species of the HAP clade are shown in their most common ecologies, illustrating the five categories of habitat preference defined in the study: (A) *Helichrysum globosum* Sch.Bip., a hemicryptophyte in swampy montane grasslands; (B) *Achryocline* spp. and (E) *Anaphalis nepalensis* (Spreng.) Hand.-Mazz., two chamaephytes growing in open high-elevation habitats, in South America and Asia respectively; (C) *H. dracaenifolium* Humbert, a macrophanerophyte from Malagasy montane forests; (D) *H. litorale* Bolus, a lowland chamaephyte in South Africa sandy environments; (F) *H. galpinii* Schltr. & Moeser, a cushion-like chamaephyte characteristic of South Africa rocky habitats. Photos credits: Mercè Galbany-Casals, except for (F) Santiago Andrés-Sánchez and (F) Simmon Attwood.

permitted all parameters to change at a specific time, also implemented in *DDD*. Each model was adjusted with an analytical correction for the sampling fraction (62 % of the clade's diversity) to address incomplete taxon sampling. The model identified as the best-fitting one had the lowest AICc score (c, for corrected AIC, which modifies the standard AIC with a correction for small sample sizes to avoid model overfitting).

Trait-dependent macroevolutionary dynamics of the HAP clade

We used the Several Examined and Concealed Trait-dependent Speciation and Extinction models implemented in the R package *SecSSE* v.3.1 (Herrera-Alsina *et al.*, 2019), to determine whether the functional trait involucral bract colour and elevational preference impacted diversification rates (independently and combined) and to estimate net diversification rates associated with the character states (H3). We did not test for the impact of life form and habitat preferences to avoid overfitting, as a high number of character states would result in an excessive number of parameters to estimate, limiting model robustness. We selected bract colour because it is often associated with pollinator attraction (highly limited in high elevations) and it can help dissipate sunlight damage (Hedberg, 1964; Lefebvre *et al.*, 2018; Baumann *et al.*, 2021; Körner, 2021). We also selected elevational range preference because it captures the habitat heterogeneity associated with mountain environments, reflecting the species' potential adaptations to specific conditions.

We fitted the following SecSSE models: (1) examined trait-dependent (ETD), (2) concealed trait-dependent (CTD) and (3) constant rate (CR), the last equivalent to a null model where diversification parameters are not associated with any trait. ETD models test for heterogeneity in diversification parameters directly associated with specific observed ('examined') traits, while CTD models assess the impact of unknown ('concealed') traits that are not directly observed but may influence diversification rates. If a CTD model provides a better fit than an ETD model, it means that the observed trait may not be the primary factor influencing diversification. Instead, other factors could potentially explain diversification patterns better. For each combination of traits, we assessed model fit using AIC.

We tested nine SecSSE models on our independent binary trait (bract colour) that had different parameters (speciation, extinction and transitions between states) estimated. All the models had two concealed states and double transitions for concealed states were disallowed to simplify the models. We allowed transition rates of the concealed states to be different from the examined trait ones (argument diff.conceal = TRUE). Since the extinction rates for all models were estimated as zero, we built two simplified models, for which extinction rates (mu) were set to zero, and the estimated transition rates were set to be the same for the examined traits and concealed traits.

To investigate the potential interactive effect of bract colour and elevational preference on diversification, we additionally tested the fit of five SecSSE models. These models had four concealed states to align with the complexity of the four examined traits (Herrera-Alsina *et al.*, 2019) that combined two bract colours with two elevational range preferences. In this case, we set the estimated transition rates to be the same for the examined traits and concealed traits (diff.conceal = FALSE), and again double transitions for concealed states were disallowed to simplify the models. Models labelled with 'full' in the name include all possible speciation (lambda, λ) and extinction (mu, μ) rates estimated, whereas those with 'L1' and 'M1' estimate just a single speciation or extinction rate, respectively. The fitted models and estimated parameters are shown in Supplementary Data Table S4.

Our SecSSE models were fitted to a phylogeny comprising 62 % of the total diversity in the HAP clade, with sampling fractions adjusted depending on the trait and state. Given that our sampling completeness was close to the lower threshold recommended for this type of analysis (Mynard *et al.*, 2023), we conducted simulations using the '*secsse_sim*' function from the SecSSE package to assess the potential impact of the sampling incompleteness on our results. We generated a total of 400 phylogenetic trees, simulating scenarios of both full (100 %) and partial (62 %) completeness. For the latter, 38 % of the tips were randomly selected and pruned to generate trees with the same level of sampling as our empirical phylogeny. The trees were simulated based on parameter values estimated from the binary trait analyses in order to minimize the number of free parameters. After fitting the full ETD and CTD models to each of the complete and randomly sampled trees, diversification rates and likelihoods were computed. The model with the best likelihood for each tree was selected, and the results from the complete and sampled trees were compared to assess the influence of sampling completeness on our conclusions.

Trait–environment convergent associations

Since we observed that certain functional traits repeatedly appeared in specific environments across the clade's distribution, we explored potential correlations between functional traits and ecological preferences to assess convergent evolution driven by trait–environment associations in the HAP clade (H4). To do so, we used BayesTraits v.4.1.2 (Pagel *et al.*, 2004, accessible at https://www.evolution.reading.ac.uk/BayesTraitsV4.1.2/BayesTraitsV4.1.2.html). Using the discrete option and an ML approach, we assessed the fit of independent and dependent models of trait-correlated evolution on our concatenated time-calibrated phylogeny. The independent model suggests that a pair of binary traits evolve independently, without impacting each other's rate of evolution. Conversely, the dependent model assumes that the rate of change in one trait is affected by the condition of the other trait. In the first case, four rate parameters are estimated (alpha0, beta1, alpha1 and beta1, where alpha represents the rate of change from 0 to 1 and beta from 1 to 0, and the numbers after alpha and beta refer to the pair of analysed traits). In the second case, transition rates (q) between trait state combinations are estimated. To determine which model best explains our data, we performed likelihood-ratio tests and compared P-values from chi-squared tests for the following trait–environment pairs: (1) strictly alpine species with white bracts; (2) cushion-like growth form with rocky habitats; (3) cushion-like growth form with montane and alpine elevational belts (separately and combined); (4) macrophanerophytes with forests habitats; (5) macrophanerophytes with humid habitats; (6) lianescent plants with forests habitats; (7) therophytes with lowlands; (8) nanophanerophytes with lowlands; and (9) hemicryptophytes with montane elevational belt (but not alpine).

RESULTS

Molecular data processing and phylogenetic analyses

Initial recovery of the 1061 COS targeted loci was near 76 % (809 loci, before paralogue filtering). We considered loci with divergence values greater than 7.91 % to be potential paralogues (Supplementary Data Fig. S1). Using the *Helichrysum*-customized reference based on our dataset, we detected an average of 222 (±59) paralogous loci per sample (Table S5). After filtering for missing data and separating alignments containing paralogues, we obtained 224 new alignments from the paralogue set. Phylogenetic inference was then performed on a total of 989 loci. The average length of aligned sequences per locus was 283 bp, with length ranging from 37 to 732 bp. Each locus contained, on average, 88 (ranging from 4 to 377) parsimony-informative sites and 129 variable sites (ranging from 5 to 453). The mean proportion of missing data was 4 %, varying from 0 to 66 % (Table S6). The concatenation of all loci produced a supermatrix consisting of 302 173 bp across 560 taxa.

The phylogenetic trees reconstructed using the concatenation (thereafter ML tree, Supplementary Data Fig. S3) and the summary-coalescent (thereafter ASTRAL tree, Fig. S4) approaches were largely congruent, with strong supports for most deeper nodes. However, topologies differed between the two methods at some intermediate and shallow nodes, particularly in the relationships involving the large polyploid genera (*Anaphalis*, *Achyrocline* and *Pseudognahalium*) and their relationships to *Helichrysum* species. Topology in these parts of the trees showed higher levels of uncertainty, often lacking statistical support. The summary-coalescence method yielded lower overall clade support, with only 51 % of the nodes achieving high support (LPP ≥ 0.95). In contrast, the ML method resulted in a higher percentage of strongly supported nodes, with 72 % according to the BS metric and 88 % based on the TBE metric (≥70 % and ≥0.7, respectively).

Divergence times and biogeographical history of the HAP clade

All divergence time estimations and 95 % confidence interval values can be found in Supplementary Data Fig. S2. The model that best fits the ancestral biogeographical range reconstruction on the ML phylogeny is DEC+j (see summary statistics in Table S7; ancestral range reconstruction in Figure S5; probabilities of ancestral areas for each node in Table S8; and node numbers in Fig. S6). The parameters retrieved with DEC+j indicate that founder-event speciation processes occurred more often than anagenetic dispersal ($j = 0.014$, $d = 0.0027$), whereas zero local extinction was inferred for the entire clade, a highly unlikely scenario. The latter result is probably the consequence of estimating extinction rates based exclusively on an extant data phylogeny. As pointed out in previous studies (Rabosky, 2010; Louca and Pennell, 2021), interpreting zero extinction rates without incorporating other data sources (especially fossil records) is problematic. BSM suggests that founder events speciation (represented by the parameter *j*) has significantly influenced the present distribution of the HAP clade (Table 1).

Consistent with previous studies (Blanco-Gavaldà *et al.*, 2025), our findings suggest that the HAP clade originated ~11.6 Ma (11.4–15.0 Ma 95 % CI), with its most probable ancestral area being a combination of lowlands and mountains in southern Africa (areas AB, 70 %). The inference of ancestral areas for nodes along the tree backbone indicates the importance of the southern African mountains (area B) as the initial centre of diversification and a repeated source of lineages that dispersed to other regions, particularly during the Pliocene. We inferred a total of 52 dispersal events from area B (Supplementary Data Table S9 summarizes all inferred dispersal event counts). Other relevant sources of dispersals were the southern African lowlands (A, 12 event counts), tropical African mountains (D, 12 event counts), the Malagasy mountains (F, 10 event counts) and the southern American mountains (L, 10 event counts). The top four dispersal sink areas are: the southern African lowlands (A, 28 event counts), tropical African mountains (D, 26 event counts; acting as source and sink), the southern African mountains (B, 14 event counts; acting as source and sink) and the Malagasy lowlands (E, 12 event counts). We found a notable asymmetry between dispersals from lowland to mountain areas and vice versa. The general trend is dispersing downward (migrating from higher elevations towards lower elevations), for which the total event count is 62. This pattern is pronounced in southern Africa and Madagascar but also observed across the Americas and between southern and tropical Africa (Fig. 3). In contrast, upward dispersals (from lowland to mountain areas) were less common (24 events), yet still substantial, indicating permeability between elevational belts. In addition to elevational shifts, long-distance dispersals between geographically distant mountain regions were also frequent (35 events on average), especially common from southern Africa to tropical Africa, from tropical Africa to Madagascar, and between North and Central America and South America (bidirectional). Dispersal events between distant lowlands were extremely rare, with an inferred average of four events.

During the Miocene, the southern African lowlands harboured a higher proportion of HAP lineages compared to the mountains (Fig. 4). However, this trend shifted progressively, with high-elevation lineages dominating by the onset of the Pliocene (5.3 Ma). This transition coincided with the expansion of lineages into regions beyond southern Africa. By the end of the Pliocene (*c.* 2.6 Ma), the mountains of tropical Africa emerged as a significant centre of diversity. During the

Table 1. Summary of biogeographical stochastic mapping (BSM) events for the HAP clade based on the DEC+j model (see all events in Supplementary Data Table S9).

Mode	Type of event	Mean (SD)	%
Within-area speciation	Sympatry	397.7 (4.2)	72.3
	Subset	21.2 (5.7)	3.9
Dispersal	Founder	92.3 (3.7)	16.9
	Range expansion	33.1 (2)	6.0
	Range contraction	0 (0)	0
Vicariance	Vicariance	5.8 (2)	1.0
Total		550 (2)	100

The average number of biogeographical events estimated for 100 BSMs are shown along with standard deviations (s.d.). Range-switching dispersals and range contractions are omitted because they were not required in the best-fitting model (DEC+j). For further information on the modes, visit http://phylo.wikidot.com/biogeobears (last accessed: 2 January 2025).

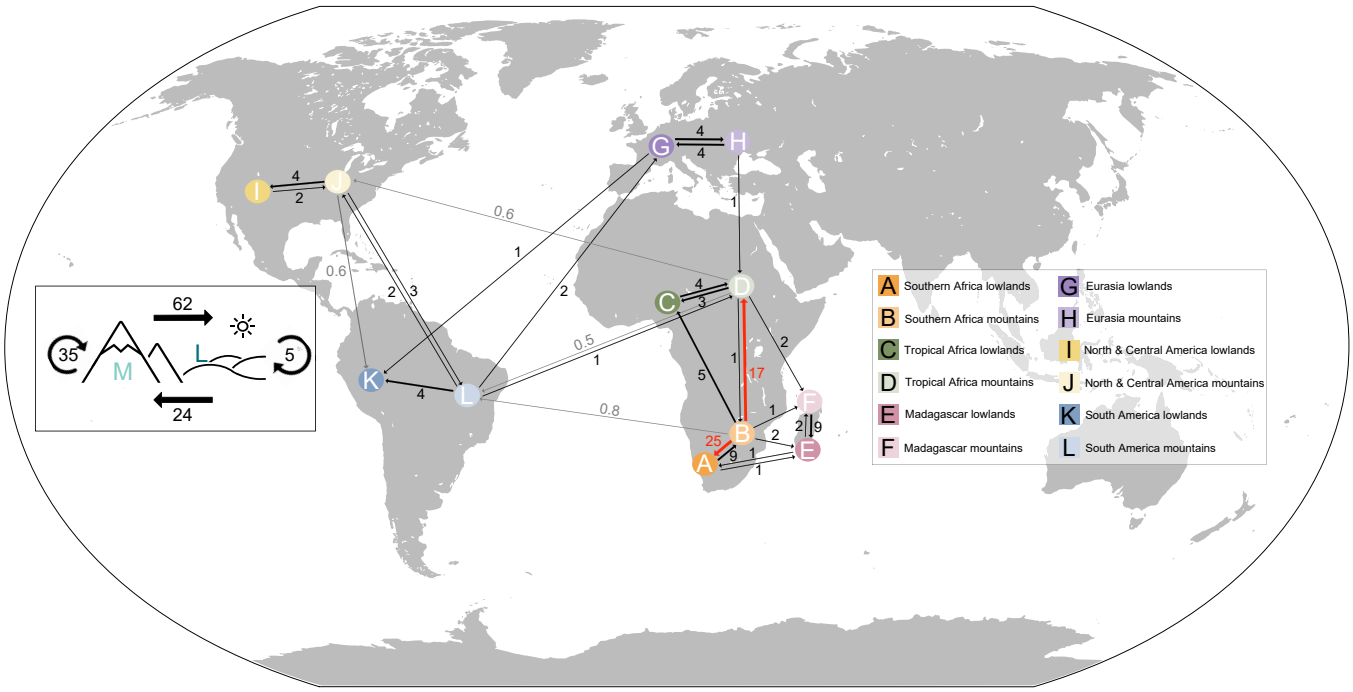

FIG. 3. Average dispersal events between regions estimated from 100 biogeographical stochastic mappings (BSMs) using the DEC+j model for the HAP clade. Arrows indicate the direction of dispersal, with numbers representing the average count of events. Arrow thickness is proportional to dispersal frequency. For readability, arrows for average counts <1 are mainly shown when connecting African areas with other continents. The thickest arrows in red show the most frequent dispersal pathways (>12 events). The inset box to the left displays the number of events involving exchanges between similar elevational belts (lowland-to-lowland/mountain-to-mountain) and transitions between distinct elevational belts (lowland-to-mountain and vice versa). Summary tables for all event counts are available in Supplementary Data Table S9.

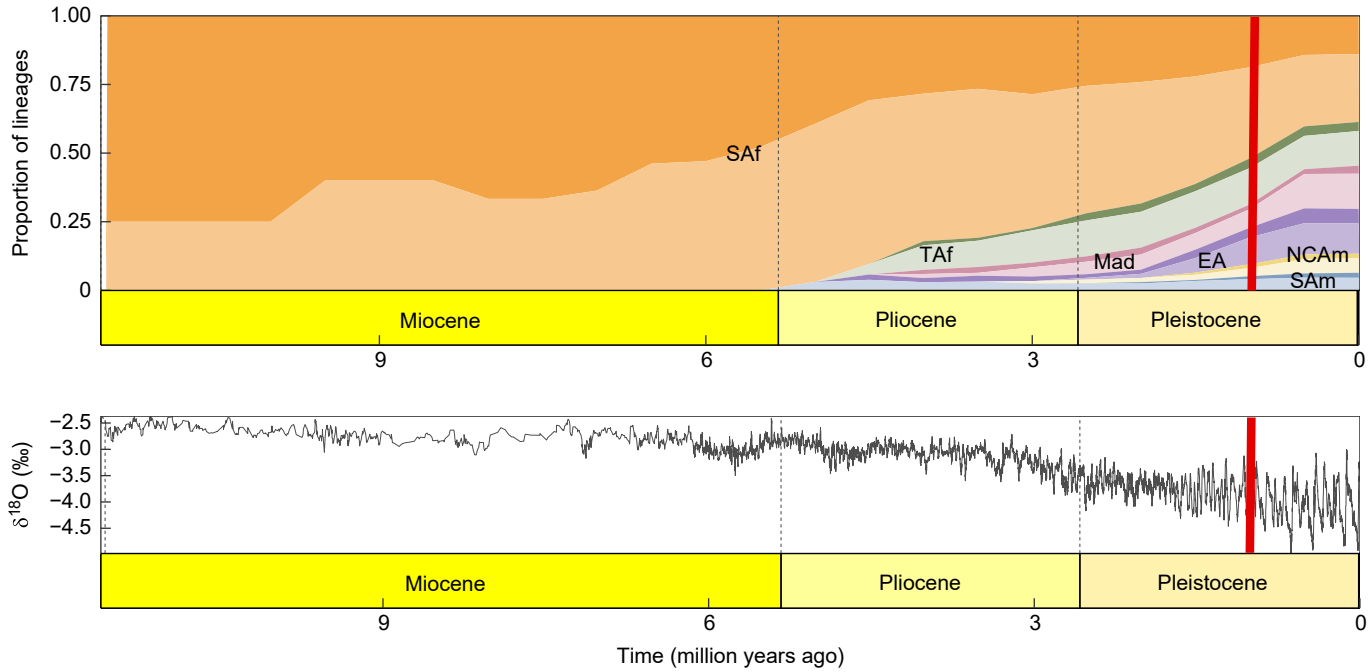

FIG. 4. Relative proportion of lineages in different biogeographical regions over time for the HAP clade, based on average dispersal counts from the biogeographical stochastic mappings (BSMs) for the DEC+j model. A large shift in net diversification rates at ~1.2 Ma is indicated in red. Biogeographical regions: SAf, southern Africa (orange); TAf, tropical Africa (green); Mad, Madagascar (pink); EA, Eurasia (violet); NCAm, North and Central America (yellow); SAm, South America (blue). For each geographical region, darker tones represent lower-elevation areas while lighter shades represent higher-elevation areas. The bottom panel shows the proxy curve for global temperature over the past 12 million years (from Zachos *et al.*, 2001).

Pleistocene, southern Africa ceased to be the primary centre of diversification of the HAP clade, giving way to young high-elevation radiations mostly outside of the African continent at *c*. 1 Ma, particularly in Madagascar, Eurasia and the Americas.

Ancestral state reconstruction of functional and ecological traits

Model selection according to AIC values indicated that the ARD model (allowing different transition rates between states) best fit the evolution of life form, elevational range and habitat preference, while involucral bract colour was better explained by equal rates (ER) or symmetrical (SYM) models (since both have the same transition rate for binary traits; see model summary tables in Supplementary Data Table S10). The ancestor of the HAP clade was reconstructed as a large shrub or small tree (macrophanerophyte) with yellow involucral bracts, occurring in sandy lowland habitats (Figs S7–S10). Over evolutionary time, alternative character states (white bracts, multiple life forms and diverse ecological preferences) emerged independently multiple times, with some reversals to the ancestral states. Significant evolutionary transitions observed include: (1) bract colour, with equal transition rates between yellow and white bracts ($q_{01} = 0.16$, $q_{10} = 0.16$); and (2) life form, where the most frequent transition involved shifts to chamaephytes, particularly from therophytes ($q_{13} = 1.62$), cushion-like forms ($q_{43} = 0.48$) and nanophanerophytes ($q_{53} = 0.24$). Other common transitions included shifts to nanophanerophytes (from lianescent forms, $q_{75} = 0.6$ and macrophanerophytes, $q_{65} = 0.28$) and to hemicryptophytes (from therophytes, $q_{12} = 0.43$ and lianescent forms, $q_{72} = 0.26$); (3) elevational range preference, downward transitions from alpine to montane belts being the most common ($q_{32} = 0.2$), with bidirectional exchanges between lowland and montane belts occurring equally ($q_{12} = 0.11$, $q_{21} = 0.11$); and (iv) habitat preference, open habitats receiving the most transitions from all other habitats types, including forests ($q_{42} = 0.48$), humid habitats, ($q_{12} = 0.45$), rocky habitats ($q_{32} = 0.28$) and sands ($q_{52} = 0.26$).

Time-, climate- and diversity-dependent macroevolutionary dynamics of the HAP clade

In RPANDA, the preferred model was a time-dependent one, with speciation and extinction rates linearly correlated with time. In DDD, the favoured one was a diversity-dependent model, indicating a major shift in diversification dynamics during the Pleistocene (*c*. 1.16 Ma). At that time, the speciation rate quadrupled, shifting from $\lambda 1 = 0.8$ to $\lambda 2 = 3.2$ speciation events per lineage per million years, while the extinction rate remained negligible ($\mu = 0$). The estimated clade's carrying capacity also more than doubled, from $K1 = 623$ to $K2 = 1370$ species (see model inference summaries in Supplementary Data Table S11). Although the RPANDA model had a slightly better fit based on AIC values, the signature of a pronounced shift in speciation rates in the Pleistocene seems evident in our dataset, explaining the position on the ranking of our second best-fitting model. Climate-dependent models had a worse fit overall, suggesting that climate alone was not the primary determinant of change in diversification dynamics.

Trait-dependent macroevolutionary dynamics of the HAP clade

Our SecSSE analyses aimed to determine whether bract colour (examined functional trait) or the interaction between bract colour and elevational preference influenced diversification within the HAP clade (Supplementary Data Table S4). In both cases, models incorporating concealed traits (CTD) provided a better fit than examined-trait-dependent (ETD) ones, as indicated by their lower AIC values. This suggests that neither the colonization of high-elevation habitats nor the acquisition of white bracts (examined traits) served as primary drivers

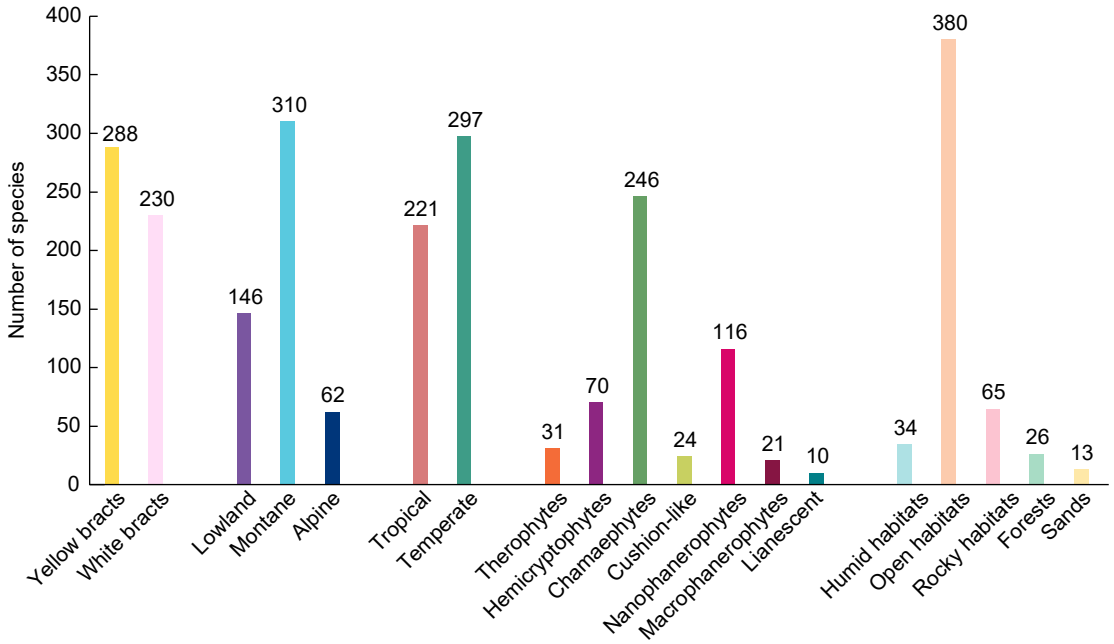

Fig. 5. Bar chart presenting the number, out of a total of 518 HAP clade taxa, of species within each of the following categories: involucral bract colour, elevational range preference, latitudinal range, life form and habitat preference. See functional trait and ecological preferences classification in Supplementary Data Table S3.

of the observed diversification patterns. Furthermore, these results are robust to the level of taxon sampling in our phylogenetic tree: simulation analyses using both fully sampled and pruned phylogenies consistently supported the same models, indicating that incomplete sampling did not bias our findings.

Trait–environment parallel associations

Our analysis of 518 ingroup taxa, representing 62 % of the HAP clade's diversity, revealed distinct patterns in character state distributions. Figure 5 illustrates the number of species in each character state (see full classification in Supplementary Data Table S3) while Fig. 6 depicts their phylogenetic distribution across the HAP clade.

Our correlation tests performed using BayesTraits showed a significant association between most pairs of character states and habitat types analysed ($P < 0.005$, Table 2). These results suggest that the presence of one state is often linked with the existence of the other, probably reflecting convergent adaptation to particular habitats found in mountain systems (full model comparison in Supplementary Data Table S12).

DISCUSSION

This study provides the most comprehensive and well-resolved phylogeny of the HAP clade to date, including representatives from across its global distribution. Our integrative approach combined data from multiple sources to test our four main hypotheses regarding the clade's diversification patterns. We confirmed a nested radiation pattern (H1), with the southern African mountains acting as the initial centre of diversification that fed other mountain systems. Our results support that long-

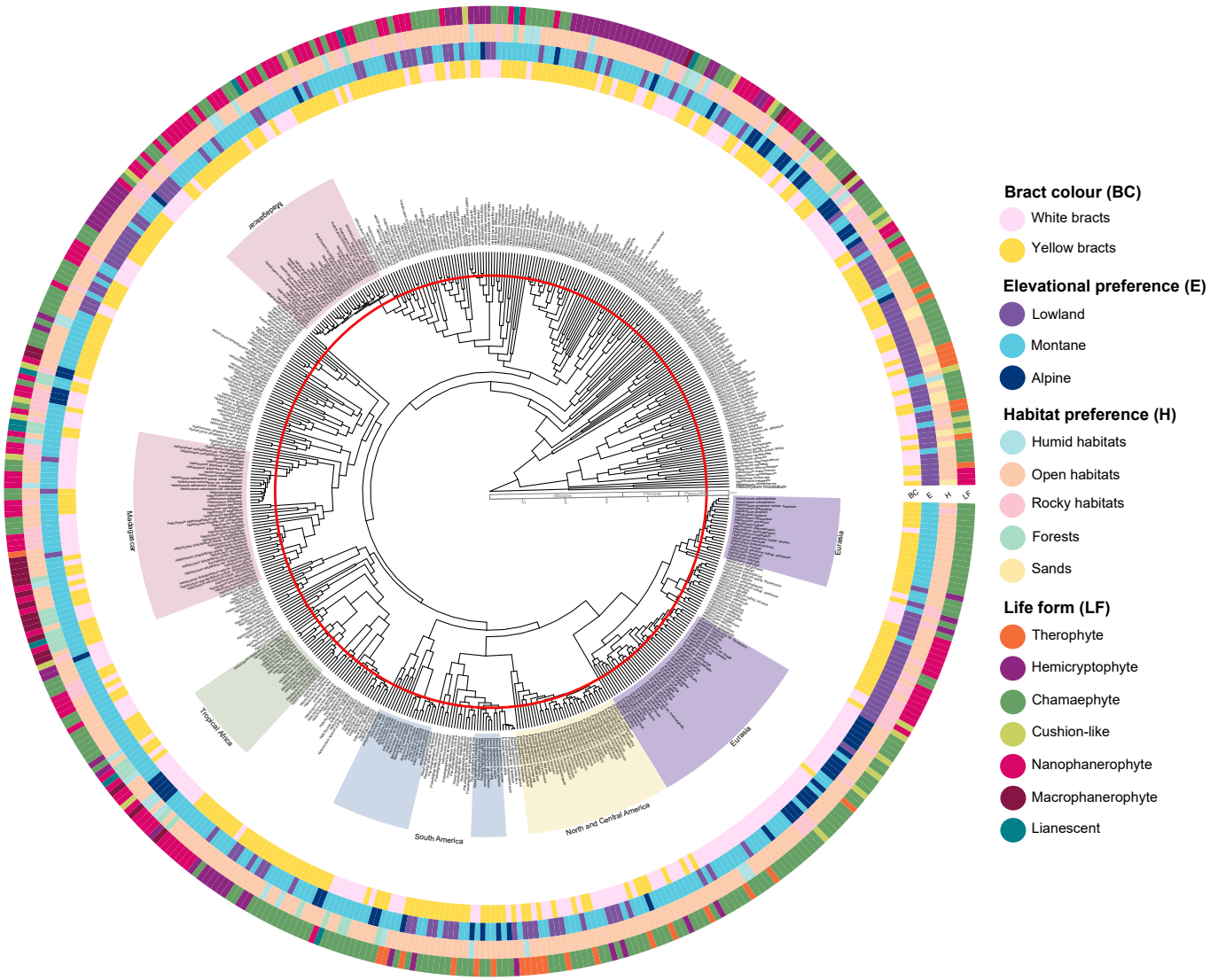

FIG. 6. Time-calibrated maximum-likelihood phylogeny of the HAP clade based on target-enrichment data generated with the probe set Compositae1061 (see Supplementary Data Fig. S2 for node ages and 95 % confidence intervals and Fig. S3 for the full tree with BS and TBE). Coloured bars on the outside of the tree in four rows (inner to outer) show the current states of each species for: involucral bract colour (BC), elevational range preference (E), habitat preference (H) and life form (LF) (see full classification in Table S3). The red line indicates the inferred diversification rate shift at ~1.2 Ma. Shaded slices on the species names indicate the main Pleistocene mountain radiations, colour-coded by biogeographical regions (geographical distribution range in Table S2).

TABLE 2. Results of correlation analyses for pairs of functional traits and ecological preferences (see classification in Supplementary Data Table S3) performed with BayesTraits, based on likelihood ratio test values.

Trait combination	*P*-value (<0.05)	Correlated
Strictly alpine – white bracts	<0.001	***
Rocky habitat – cushion-like growth	<0.001	***
Strictly montane – cushion-like growth	<0.001	***
Strictly alpine – cushion-like growth	<0.001	***
High elevation (combination of montane and alpine) – cushion-like growth	0.08	No
Forest habitats – macrophanerophytes	<0.001	***
Humid habitats – macrophanerophytes	<0.001	***
Forest habitats – lianescent forms	<0.001	***
Lowland – therophytes	<0.001	***
Lowland – nanophanerophytes	<0.001	***
Strictly montane – hemicryptophytes	<0.001	***

Positively correlated trait–environment combinations are indicated as follows: ***$P < 0.001$; **$P < 0.01$; *$P < 0.05$; non-correlated trait combinations are in bold grey (full results in Supplementary Data Tables S1 and S2).

distance dispersal repeatedly occurred among geographically distant mountain regions (H2). Multiple colonizations from high- to low-elevation habitats indicate significant elevational permeability. Pleistocene climatic oscillations probably played a crucial role in promoting regional allopatric speciation, as there was a notable rise in the net diversification rate during this period, which coincides with the emergence of young radiations within several mountain regions. In contrast to our expectation of key traits driving radiations, trait-dependent speciation and extinction analyses with SecSSE suggest that increased diversification rates in high-elevation environments are not associated with the acquisition of white bracts (H3). Instead, adaptability and niche lability seem to have contributed to local-scale diversification, as indicated by positive evolutionary correlations between functional traits and specific environmental preferences (H4), linked to microhabitat specialization (H2). The wide geographical distribution and diversity of trait combinations paired with the varied ecological preferences of the HAP clade suggests a complex evolutionary history.

High-elevation environments as sources and sinks of plant diversity

Our findings indicate that the HAP clade emerged in southwestern Africa in the Mid-Miocene (*c.* 11 Ma), aligning with the onset of global cooling and heightened seasonality, which replaced warmer subtropical conditions (Herbert *et al.*, 2016; Westerhold *et al.*, 2020). In particular, southwestern Africa experienced increased aridity and transitioned to a winter rainfall pattern, driven by the establishment of the westerly wind system and the intensification of the Benguela current (Roberts *et al.*, 2014; Neumann and Bamford, 2015). As temperatures fell, the proportion of southern African high-elevation HAP clade species increased (Fig. 4) alongside the expansion of savannas and grasslands (Linder, 2003; Dupont *et al.*, 2013), the latter determined by high-elevation cold conditions rather than drought in southern Africa (see Bredenkamp *et al.*, 2002). In addition to pronounced global cooling, this period was marked by intense mountain uplift in eastern Africa, affecting the Great Escarpment, the Drakensberg and the mountains along the Rift (Partridge, 1998; Partridge and Maud, 2000; Sepulchre *et al.*, 2006), driving significant biotic turnovers (Herbert *et al.*, 2016). High-elevation HAP species started to dominate around the Miocene–Pliocene boundary with dispersals to tropical Africa, leading to the occupation and diversification in even higher mountains (Fig. 4), eventually colonizing mountain systems on other continents in the Pleistocene (Fig. 3).

The concept of nested radiation (Linder, 2014; Linder and Verboom, 2015) refers to the idea that regionally rich floras are often the result of multiple, interconnected radiations that have proliferated in different ecological settings. These radiations influence each other through cross-seeding, where clades from one radiation spawn subclades in another, creating a complex, interconnected network of diversification. The accumulation of diversifying lineages over time can potentially spread to other continents, becoming a source of global biodiversity. Linder and Verboom (2015) point to the northern Andes region as a super-radiation, as it is surrounded by multiple contrasting ecological settings and provides gradual environmental change. Our findings support and extend the concept of nested evolutionary radiations described for southern African lineages (Linder, 2014; Linder and Verboom, 2015), demonstrating that the pattern can be generalized to mountain systems worldwide.

Differences in clade ages, species richness and distribution patterns suggest that the southern African montane grasslands served as ancestral centre of diversification and source of pre-adapted high-elevation lineages (Donoghue, 2008). In contrast, mountains in the Americas, Eurasia and Madagascar acted primarily as sinks (Fig. 3; Supplementary Data Table S9), harbouring younger and smaller radiations, with rapid accumulation of species occurring during the Pleistocene (Grytnes and McCain, 2007; Rahbek *et al.*, 2019). Our biogeographical reconstruction reveals multiple instances of allopatric speciation driven by lineage dispersal between bioclimatically similar but distant mountain systems (Fig. 3). This pattern, previously observed at smaller scales for Malagasy *Helichrysum* (Blanco-Gavaldà *et al.*, 2025), highlights the role of niche conservatism (Wiens and Graham, 2005; Wiens *et al.*, 2010) in shaping global HAP clade distributions. Notably, high-elevation regions also served as a source of lineages for lower elevations, probably due to niche displacements during climatic fluctuations (Chala *et al.*, 2017; Flantua *et al.*, 2019), which eventually fostered niche shifts and subsequent specialization (Donoghue and Edwards, 2014). This dynamic is reflected in a high permeability across elevational belts, with multiple recent colonizations of lowland regions throughout the clade's distribution, highlighting the ecological lability of HAP species and placing mountain systems worldwide as a source of lowland diversity. While upward shifts from low- to high-elevation habitats are more common in the literature, for instance in *Espeletia* (Monasterio and Sarmiento, 1991), *Androsace* (Boucher *et al.*, 2012), *Bulbophyllum* Thouars (Gamisch *et al.*, 2016) and *Saxifraga* L. (Carruthers *et al.*, 2024), as well as in some butterflies (Chazot *et al.*, 2016) and birds (Roy, 1997;

García-Moreno *et al.*, 1998), downward transitions also occur, such as those in *Dendrosenecio* (Knox and Palmer, 1995) and certain butterflies (Elias *et al.*, 2009) and birds (Sedano and Burns, 2010, Van Els *et al.*, 2021). These migrations across the elevational gradient were probably driven by pre-existing adaptations, such as tolerance to high insolation and hydric stress (Donoghue, 2008; Edwards and Donoghue, 2013), considering that HAP clade species predominantly inhabit open habitats (Figs 5 and 6) and that the transitions in both directions (from high to low elevations and vice versa) were gradual rather than extreme. For example, shifts typically occurred between alpine and montane environments or between montane and lowland habitats.

Pleistocene climate oscillations triggered parallel mountain radiations in the HAP clade

The evolutionary history of the HAP clade seems to be profoundly influenced by climate oscillations. The clade's expansion and radiation outside of Africa coincided with the onset of extreme glacial–interglacial cycles characteristic of the Mid-Pleistocene Transition *c.* 1.2 Ma (Clark *et al.*, 2006). This timing aligns with our inference of a four-fold increase in the net diversification rate of the clade (Fig. 4; Supplementary Data Table S11). As mentioned previously, these climatic fluctuations probably caused cycles of connectivity and isolation, driving major range expansions and contractions (Flantua *et al.*, 2019). This dynamic facilitated the regional dispersal/migration of lineages preadapted to cool and dry conditions and the isolation or secondary contact of populations following elevational shifts of preferred climatic conditions. The formation of extensive continental ice sheets, mainly in the Northern Hemisphere and across the highest mountains worldwide, induced important environmental changes (Westerhold *et al.*, 2020), forcing lineages to face extinction if they were unable to adapt *in situ* or did not successfully colonize other regions through dispersal (Graae *et al.*, 2018). The timing and environmental shifts associated with the Mid-Pleistocene Transition probably served as the primary driver of extensive diversification in Eurasian HAP lineages (Mediterranean, Asian and Macaronesian *Helichrysum* and Asian *Anaphalis*) as well as in the American lineages (*Achyrocline* and *Pseudognaphalium*). In Africa and Madagascar, glacial stages contributed to the expansion of cold ecosystems and increased connectivity between mountain ranges. This facilitated the descent and expansion of high-elevation lineages, both alpine and montane, with a stronger impact on the latter (Kebede *et al.*, 2007; Chala *et al.*, 2017). Similar processes have been documented in the Andes (Flantua *et al.*, 2019) and the Guayanan tepuis (Rull, 2005). In African and Malagasy high-elevation lineages, these dynamics left a strong signature of allopatric speciation, exemplified by narrowly endemic species restricted to specific massifs, such as *Helichrysum brownei* S.Moore in Mt Kenya, as well as widespread taxa spanning multiple mountains across tropical Africa, a result of recent reconnections, such as in *Helichrysum formosissimum* Sch.Bip. The species *Helichrysum arwae* J.R.I.Wood, a cushion-like chamaephyte in rocky habitats of Yemeni mountains, which is sister species to *Helichrysum horridium* Sch.Bip., a nanophanerophyte in open Ethiopian habitats, provide clear examples of allopatric speciation in mountain habitats (Fig. 6). A similar pattern is observed in Madagascar, where several clades contain mountain-endemic species, such as *Helichrysum vaginatum* Humbert, found in several summits of the southeastern mountains, and its sister species, *Helichrysum marojejyense* Humbert, restricted to the summit of Mt Marojejy in the northeast (Humbert, 1962).

Recent studies suggest that speciation mechanisms are often interconnected, typically starting with an allopatric phase followed by ecological divergence, shaping macroevolutionary dynamics through both trait retention and trait changes (e.g. Aguilée *et al.*, 2018; Gorel *et al.*, 2022; Blanco-Gavaldà *et al.*, 2025; Gorospe *et al.*, 2025). Our findings align with the diversification patterns reported for *Veronica* sect. *Hebe* in New Zealand's mountains (Thomas *et al.*, 2023). The lability of the HAP clade, which allowed for high permeability across heterogeneous habitats, combined with the ability to persist and diversify in mountains favoured by climate oscillations, makes the clade fit the three stages of mountain diversification proposed in Thomas *et al.* (2023). Specifically for the HAP clade, it started with long-distance dispersal from similar biomes, which provides preadapted colonizers (this would include both regional and local allopatric speciation). The first stage was followed by *in situ* speciation associated with ecological specialization, rather than the acquisition of key innovations. Finally, the latest stage concluded with niche transitions, usually down the slope, which can be considered a second round of colonization.

The history of a dynamic and highly adaptable group: heterogeneity within the HAP clade

Our trait-dependent speciation and extinction analyses with SecSSE revealed that models incorporating concealed traits provided a better fit than those where our examined states (bract colour and elevational range) affected diversification, indicating that unknown factors explain differences in net diversification rates across the HAP lineages (Supplementary Data Table S4). These results align with other studies showing that certain floral features might not directly drive rapid radiations (e.g. *Helianthemum*, Martín-Hernanz *et al.*, 2023). While it is unclear whether other key innovations contributed to increased diversification rates in high-elevation species, the complex interplay between diverse trait combinations within the lineage and the heterogeneous environmental conditions across elevational and latitudinal gradients where the HAP clade occurs probably points to a more complex evolutionary pattern (see Fig. 6).

Correlation analyses (Supplementary Data Table S12), although not indicating increased diversification rates, suggest associations between the evolution of functional traits (bract colour and life form) and ecological preferences (elevation and habitat preferences). Specifically, we found that the evolution of white bracts was associated with colonization of higher elevations, where pollinator availability typically decreases (e.g. Blionis and Vokou, 2001). In such environments, larger and more intensely white flowers attract generalist pollinators, primarily Diptera (Lefebvre *et al.*, 2018; Baumann *et al.*, 2021; Körner, 2021). These larger flowers (capitula or aggregations of capitula, in the case of Compositae) not only enhance visibility but also retain warmth, providing pollinators with a warmer resting surface in addition to a food source

(Dietrich and Körner, 2014). Furthermore, shiny white bracts might have also been positively selected for their capacity to reflect harmful UV radiation (Hedberg, 1964; Körner, 2021).

Members of the HAP clade show a strong preference for open habitats (Supplementary Data Fig. S9), which regardless of elevation are devoid of tree cover and generally more exposed to climatic adversities. Plants in such environments often exhibit shorter statures (predominantly chamaephytes), an adaptation to water scarcity (Körner, 2021). Extreme forms include cushion-like chamaephytes, which dominate rocky high-elevation environments (Fig. 6; Tables S3 and S12). In contrast, larger arborescent forms tend to occupy more stable and humid environments, such as montane forests, streamside habitats, or valleys and gullies (Körner, 2021, and in the HAP clade, see Fig. 6; Tables S3 and S12). These life form–habitat associations detected in the HAP clade (Table 2; Fig. 6) highlight how contrasting ecological niches within mountain systems promote diversification through ecological speciation, with steep elevational gradients creating a mosaic of microhabitats in close proximity, while remaining in the same broad-scale bioclimatic zones (Doebeli and Dieckmann, 2003; Jones *et al.*, 2011; Winkler *et al.*, 2016; Antonelli *et al.*, 2018; García *et al.*, 2020). Such local-scale adaptations and specialization to microhabitats have probably contributed to diversification in mountainous regions, as demonstrated in European mountain systems (Smyčka *et al.*, 2022). Microhabitat-driven speciation is illustrated by several pairs of sister taxa from our study, for example, the afroalpine sister species *Helichrysum newii* Oliv. & Hiern, a widespread nanophanerophyte common in high-elevation open habitats of eastern tropical Africa, coexisting with the partly sympatric *Helichrysum chionoides* Philipson, a macrophanerophyte restricted to humid habitats in Mt Aberdare and Mt Kenya, similar to the case of ecological speciation reported for two sympatric species of *Dendrosenecio* in Mt Kenya in Gorospe *et al.* (2025) and the case of parapatric speciation across the elevational gradient in Madagascar, where two morphotypes of *Helichrysum dracaenifolium* Humbert coexist in Mount Marojejy, one a nanophanerophyte inhabiting open areas at 1550–1870 m and the other a macrophanerophyte restricted to forests at 1150–1600 m.

Ancestral state reconstructions (Supplementary Data Figs S7–S10) reflect a history of high adaptability and evolutionary dynamism in the HAP clade, with certain traits evolving independently multiple times across the phylogeny. The predominance of high-elevation perennial woody species (Figs 5 and 6) mirrors the well-documented evolutionary history of *Lupinus* (Fabaceae) in the New World (Hughes and Eastwood, 2006; Drummond, 2008). Woodiness has similarly been identified as a key innovation in other angiosperm mountain lineages, including *Alchemilla* in Africa (Gehrke *et al.*, 2016), *Lachemilla* Rydb. in the Andes (Morales-Briones *et al.*, 2018) and Delphinieae in the Himalayas (Jabbour and Renner, 2012). Nürk *et al.* (2019 and references therein) have shown the central role of disparity of growth forms in adaptive radiations on oceanic and tropical sky islands. The diversification of life forms observed in the HAP clade, particularly in tropical Africa and Madagascar (but not in Eurasia or the Americas, Fig. 6), supports the idea that adopting diverse life forms is a key ecological strategy for thriving at high elevations (Hedberg, 1964; Hedberg and Hedberg, 1979; Körner, 2021). Interestingly, woody forms also dominate in lowland environments, since only a small proportion of HAP species are therophytes or hemicryptophytes (Fig. 5). Ancestral state reconstructions suggest that the clade's ancestor was a macrophanerophyte (Fig. S10) adapted to the arid regions of southern Africa, consistent with links between the evolution of woodiness and palaeoclimatic aridification (Hooft van Huysduynen *et al.*, 2021; Zizka *et al.*, 2022). Despite its origins in arid regions, this life form became dominant in tropical mountains and humid habitats.

Despite detecting a wide variation in traits linked to heterogeneous mountain habitats, trait evolution alone does not fully explain the HAP clade's rapid diversification during the Pleistocene. Other factors not considered in this study, such as ploidy (Combrink *et al.*, 2025), may be important in explaining high-elevation radiations as observed in *Myosotis* Hill (Meudt *et al.*, 2025). The HAP clade is also a lineage shaped by a history of hybridization and polyploidy, with known allopolyploid subclades predominantly in Eurasia and the Americas (Galbany-Casals *et al.*, 2004; Galbany-Casals and Romo, 2008; Smissen *et al.*, 2011; Galbany-Casals *et al.*, 2014; Acosta-Maindo *et al.*, 2018). The origin of these subclades may be closely tied to polyploid speciation, often associated with the colonization of new territories (e.g. Ramsey, 2011; Carnicero *et al.*, 2017) and genomic plasticity that provides resilience and adaptability (Barker *et al.*, 2016; Godfree *et al.*, 2017; Van de Peer *et al.*, 2017, 2021). It is positively correlated with latitude (Rice *et al.*, 2019) and has been shown to drive diversification in high-elevation and climatically unstable regions (Meudt *et al.*, 2021), such as the Andes (Luebert and Weigend, 2014), the Pan-Himalayas (Wen *et al.*, 2014) and European mountains (Pachschwöll *et al.*, 2015; Slovák *et al.*, 2023). Many polyploid species originated during the Pleistocene (Novikova *et al.*, 2018; Han *et al.*, 2022), probably driven by range contractions and reconnections that facilitated hybrid speciation (Folk *et al.*, 2024). Polyploidy also contributes to morphological and ecological diversity (Baniaga *et al.*, 2020), with habitat shifts influenced by microclimatic factors playing a crucial role in polyploid evolution (Marchant *et al.*, 2016). Future research is needed to specifically investigate the impact of hybridization and polyploidy on diversification patterns in the HAP clade, particularly regarding high-elevation radiations in Eurasia and the Americas.

CONCLUSIONS

This study of the evolutionary history of the HAP clade provides valuable insights into the assembly of high-elevation floras, highlighting the dual role of mountain systems as both sources and sinks of biodiversity. The diversification and distribution patterns of the HAP clade reflect the complex interplay of several factors, particularly related to climate and ecological adaptation, operating across various temporal and spatial scales. The clade's evolutionary success lies in its remarkable long-distance dispersal capacity and ability to colonize new regions as well as adaptability, being able to move across elevational gradients and thrive in different habitats, undergoing repeated radiations. While *in situ* diversification is most evident in mountain systems, it also occurred at lower elevations. Our findings suggest that Pleistocene climatic fluctuations played a key role in recent parallel mountain radiations. These oscillations

promoted range expansions and contractions, leading to cycles of isolation and reconnection between populations. Such dynamics probably fostered allopatric speciation at both regional and local scales, evident in the emergence of numerous regional endemics confined to specific massifs or regions, often constituting morphologically homogeneous clades. At a local scale, ecological speciation emerged as a significant driver of diversification. This is particularly evident in the parallel acquisition of life forms that enabled adaptation to specific microhabitats across different mountain massifs. The independent evolution of these traits within heterogeneous environments fostered niche differentiation, with African and Malagasy lineages showing especially diverse morphologies and ecological preferences. Although we did not consistently observe a clear association between functional traits and increased diversification rates at broader scales, our results indicate that niche lability was key in facilitating local-scale adaptations, potentially driving diversification within specific mountain systems. In contrast, the evolutionary trajectories of Eurasian and American radiations remain less clear but may involve polyploidization and hybridization, processes that enhanced genomic plasticity and resilience to climatic fluctuations. The HAP clade exemplifies how lineages can successfully persist and diversify in challenging high-elevation environments through flexible evolutionary strategies, combining dispersal, specialization to microhabitats and genomic plasticity. These findings contribute to the understanding of diversification patterns in species-rich lineages inhabiting mountain systems worldwide.

FUNDING

This research received funding from the Spanish Ministry of Science, Innovation and Universities (PD2019-105583GB-C22/AEI/10.13039/501100011033) as well as from the Catalan Agency for Management of University and Research Grants through the ‘Ajuts a grups consolidats’ programme (2021SGR00315) and the PhD grant "FI-AGAUR" (2022FI_B00150 awarded to C.B.-G).

ACKNOWLEDGEMENTS

We express our gratitude to María Luisa Gutiérrez for technical support throughout the laboratory processes, as well as to the curators and technicians of the herbaria who contributed material for this study, along with all collaborators who shared material from their own collections. We appreciate the assistance of Sebastián Arrabal and Marta Kandziora during fieldwork in Madagascar and Rwanda, respectively. We acknowledge the Direction des Aires Protégées, des Ressources Naturelles renouvellables et des Ecosystèmes and the Madagascar National Parks in Madagascar for granting collecting permits to M.G.-C. and S.G.R.; Parc Botanique et Zoologique de Tsimabazaza; Missouri Botanical Garden, Madagascar; and particularly Faranirina Lantoarisoa for logistical support and facilitating collecting permits for M.G.-C. and S.G.R. We extend our gratitude to Rokiman Letsara for his assistance during fieldwork in Madagascar and coordinating logistics on the ground. Collection in Rwanda was conducted under Research permit No. NCST/482/304/2022 and with authorization from the Rwanda Development Board (RDB) Tourism and Conservation to collect in the Volcanoes National Park. We are grateful to Professor Elias Bizuru for permitting the affiliation of M.G.-C. and J.A.C. with the University of Rwanda, and to Dr Richard Muvunyi from RDB for his support. We also thank the team at the Volcanoes National Park for their field assistance as well as Beth Kaplin and the staff from the National Herbarium of Rwanda, as along with the personnel at the Ellen DeGeneres Campus in Musanze for logistical support. The collection in South Africa was carried out under research permits CN35-28-23663 (Western Cape Nature Conservation Board) and HO/RSH/47/2021 (Province of Eastern Cape, Economic Development, Environmental Affairs & Tourism). Additionally, we extend our thanks to Arne Anderberg for helping with the identification of some specimens from Madagascar, Qin Tian for assisting with the use of the ltstR package, John Clarke for insightful suggestions on methodology, and Simmon Attwood and Deon du Plessis for providing images of some South African *Helichrysum*.

SUPPLEMENTARY DATA

Supplementary data are available at *Annals of Botany* online and consist of the following. Figure S1: Pairwise distance histogram from ParalogWizard showing the distribution of pairwise distances between exonic contigs for each locus (in divergence percentages, 7.9–20.3 %). Dashed lines indicate mean divergence values for each peak, and standard deviation (minus and plus sigma) values are provided in the legend. Figure S2: Dated maximum-likelihood phylogeny of the HAP clade generated with RelTime implemented in MEGA 11. Blue numbers next to the nodes show mean ages (above) and grey numbers show 95 % confidence intervals (below). Calibration points are indicated to the left of the nodes. Figure S3: Maximum-likelihood phylogeny (RAxML-NG) of the HAP clade based on nuclear DNA loci generated with the target-enrichment probe set Compositae1061. Node support values are indicated: BS (in blue, above) and TBE (in red, below). Figure S4: ASTRAL species tree of the HAP clade based on nuclear DNA loci generated with the target-enrichment probe set Compositae1061. Numbers next to the nodes indicate local posterior probabilities (LPP). Figure S5: Ancestral biogeographical range inference of the HAP clade using the best-fitting model DEC+j. It is based on a time-calibrated phylogeny generated under the concatenation approach using target-enrichment data (Compositae1061 probe set). Pie charts at nodes show the relative probability of the possible states. Primary colours indicate single areas; grey denotes area combinations. The shift in net diversification rates is marked in red (∼1.2 Ma). Coloured squares indicate the main Pleistocene mountain radiations. Figure: S6. Node numbers on a time-calibrated phylogeny of the HAP clade generated under the concatenation approach using target-enrichment data (Compositae1061 probe set). These node numbers correspond to those in the ancestral range probabilities table (Supplementary Data Table S6). Figure S7: Ancestral state reconstruction analysis for bract colour evolution in the HAP clade based on a time-calibrated ML tree generated with target-enrichment data (Compositae1061 probe set). Pie charts on tree nodes indicate the probability of the most likely ancestral morphology. Circles next to the tips are coloured according to the current morphotype of each species. Figure S8: Ancestral state reconstruction analysis for elevational range preference evolution

in the HAP clade based on a time-calibrated ML tree generated with target-enrichment data (Compositae1061 probe set). Pie charts on tree nodes indicate the probability of the most likely ancestral elevational range. Circles next to the tips are coloured according to the current preference of each species. Figure S9: Ancestral state reconstruction analysis for habitat preference evolution in the HAP clade based on a time-calibrated ML tree generated with target-enrichment data (Compositae1061 probe set). Pie charts on tree nodes indicate the probability of the most likely ancestral habitat. Circles next to the tips are coloured according to the current preference of each species. Figure S10: Ancestral state reconstruction analysis for growth form evolution in the HAP clade based on a time-calibrated ML tree generated with target-enrichment data (Compositae1061 probe set). Pie charts on tree nodes indicate the probability of the most likely ancestral morphology. Circles next to the tips are coloured according to the current morphotype of each species. Table S1: List of studied materials, including herbaria codes and voucher information. BioSample accession numbers are provided for each specimen (accessible at https://www.ncbi.nlm.nih.gov/sra). Samples taken from other studies are associated with the following BioProjects: Blanco-Gavaldà *et al.*, 2023, BioProject PRJNA936872; Blanco-Gavaldà *et al.*, 2025, BioProject PRJNA1121119; Mandel *et al.*, 2019, BioProject PRJNAS40287; and Schmidt-Lebuhn and Bovill, 2021, BioProject PRJNA665592. Table S2: Geographical distribution of HAP clade species for biogeographical ancestral state reconstruction analyses with BioGeoBEARS. The first row lists the 12 biogeographical areas defined in the study with their corresponding letter codes in parentheses. Table S3: Functional trait (bract colour and life form) and ecological preference (elevation and habitat) classification table for HAP clade species. Table S4: Summary of the defined SecSSE models and parameter estimates. The best-fitting models, identified by the highest AIC scores, are highlighted in bold. Abbreviations: L (lambda, speciation rate); M (mu, extinction rate); Q (transition rate); LL (likelihood); k (number of parameters); AIC (Akaike Information Criterion). Model types: ETC (examined trait-dependent); CTD (concealed trait-dependent); CR, (constant rate). Variations: full (all possible speciation and extinction rates are estimated); L1 (a single speciation rate is estimated); M1 (a single extinction rate is estimated); simple (extinction rate fixed at 0). Table S5: Statistics from paralogy analyses using ParalogWizard. For each sample, the number of paralogue loci within the selected divergence threshold (7.9–20.4 %) is provided. Table S6: Summary statistics of the selected loci (including paralogues) after filtering for missing data for subsequent phylogeny reconstruction (script HPM5). Table S7: Summary statistics of biogeographical model testing in BioGeoBEARS. Likelihood scores (LnL), corrected Akaike Information Criterion (AICc) and free parameter values are detailed. Parameters include: dispersal (d), extinction (e) and founder-event (j). The best-fitting model (DEC+j) is highlighted in bold. Table S8: Ancestral range probabilities for the HAP clade on the DEC+j model, corresponding to the pie charts in Supplementary Data Fig. S5. The first column contains node numbers from Fig. S6. Table S9: Average number of dispersal events estimated in the history of the HAP clade using 100 biogeographical stochastic mappings under the DEC+j model. Counts are averaged across and standard deviations are provided below each table. Rows represent source areas and columns the sink areas. Cell colours indicate event frequency (red: highest to green: lowest). Additional tables summarize exchanges between similar elevational belts (lowland-to-lowland, mountain-to-mountain) and transitions between bioclimatically distinct elevational belts (lowland-to-mountain and vice versa), reflecting broad-scale niche conservatism and niche shifts. Table S10: Summary of the fitted models for ancestral state reconstruction for two functional traits (bract colour and life form) and two ecological preferences (elevation and habitat). Model abbreviations correspond to: ER, model with all rates equal; ARD, model with different transition rates for all possible transitions; SYM, symmetrical model in which rates between any two states do not differ. The best-fitting model according to AIC is indicated in bold. Table S11: Summary of the fit of various diversification models applied to the HAP clade's phylogeny. The best-fitting model based on AICc is highlighted in bold and green. Abbreviations: NP (number of free parameters); logL (log-likelihood); AICc (corrected AIC scores); lambda (speciation rate); alpha (rate of variation in speciation over time or with temperature, depending on the model); mu (extinction rate); K (carrying capacity in diversity-dependent models); beta (rate of variation of extinction over time or with temperature, depending on the model). Table S12: Maximum likelihood correlation tests on pairs of binary traits (functional trait vs. ecological preference) performed with BayesTraits. The independent model (four rate parameters, alpha1, beta1, alpha2, beta2) assumes traits evolve independently on the phylogenetic tree, while the dependent model (eight rate parameters) assumes correlated evolution, where the rate of change in one trait depends on the state of the other (transition rates, q). In the dependent model, double transitions are set to zero. Likelihood ratio (LR) tests were used to compare model likelihoods (Lh), and significance was assessed from chi-squared tests (*P*-values). Probabilities for the root being in specific state combinations are also indicated. References: List of reference floras and online resources consulted for extracting geographical range distribution (Table S2), functional trait data and ecological preference data (Table S3) used to classify the studied HAP clade species.

DATA AVAILABILITY

The list of studied materials including herbaria codes, voucher information and BioSample accession numbers (accessible at https://www.ncbi.nlm.nih.gov/sra) is available in Supplementary Data Table S1. The geographical range distribution classification is available in Table S2 and the functional trait and ecological preferences classification in Table S3.

AUTHOR CONTRIBUTIONS

C.B.-G.: conceptualization, resources, methodology, investigation, formal analyses, data curation, visualization, writing original draft. R.E.O.: conceptualization, investigation, supervision; writing – reviewing and editing. L.V.: conceptualization, investigation, supervision; writing – reviewing and editing. T.J.: software, validation, writing – reviewing and editing. S.A.-S.: methodology, resources, data curation, investigation, writing – reviewing and editing. N.B.: resources, methodology, writing – reviewing and editing. J.A.C.: resources,

investigation, writing – reviewing and editing. P.C.: resources, writing – reviewing and editing. O.C.: investigation, data curation, writing – reviewing and editing. G.V.C.: resources, writing – reviewing and editing. F.L.: resources, writing – reviewing and editing. L.D.M.: software, validation, writing – reviewing and editing. G.P.-S.: resources, investigation, formal analysis, data curation, writing – reviewing and editing. S.G.R.: resources, writing – reviewing and editing. A.S.: conceptualization, methodology, resources, funding acquisition, project administration, writing – reviewing and editing. C.R.: conceptualization, methodology, investigation, formal analyses, data curation, supervision, writing – reviewing and editing. M.G.C.: conceptualization, resources, methodology, investigation, formal analyses, data curation, supervision, writing – reviewing and editing, project administration, funding acquisition.

REFERENCES

Acosta-Maindo A, **Hinojosa-Espinosa O**, **Galbany-Casals M. 2018**. Polyploidy and new chromosome counts in *Pseudognaphalium* Kirp. (Compositae: Gnaphalieae). *Caryologia* **71**: 471–481. doi:10.1080/00087114.2018.1503501

Aguilée R, **Gascuel F**, **Lambert A**, **Ferriere R. 2018**. Clade diversification dynamics and the biotic and abiotic controls of speciation and extinction rates. *Nature Communications* **9**: 3013. doi:10.1038/s41467-018-05419-7

Anderberg AA. 1991. Taxonomy and phylogeny of the tribe Gnaphalieae (Asteraceae). *Opera Botanica* **104**: 1–195.

Antonelli A. 2015. Biodiversity: multiple origins of mountain life. *Nature* **524**: 300–301. doi:10.1038/nature14645

Antonelli A, **Kissling WD**, **Flantua SGA**, ***et al.* 2018**. Geological and climatic influences on mountain biodiversity. *Nature Geoscience* **11**: 718–725. doi:10.1038/s41561-018-0236-z

Baniaga AE, **Marx HE**, **Arrigo N**, **Barker MS. 2020**. Polyploid plants have faster rates of multivariate niche differentiation than their diploid relatives. *Ecology Letters* **23**: 68–78. doi:10.1111/ele.13402

Bankevich A, **Nurk S**, **Antipov D**, ***et al.* 2012**. SPAdes: a new genome assembly algorithm and its applications to single-cell sequencing. *Journal of Computational Biology* **19**: 455–477. doi:10.1089/cmb.2012.0021

Barker MS, **Arrigo N**, **Baniaga AE**, **Li Z**, **Levin DA. 2016**. On the relative abundance of autopolyploids and allopolyploids. *The New Phytologist* **210**: 391–398. doi:10.1111/nph.13698

Baumann K, **Keune J**, **Wolters V**, **Jauker F. 2021**. Distribution and pollination services of wild bees and hoverflies along an altitudinal gradient in mountain hay meadows. *Ecology and Evolution* **11**: 11345–11351. doi:10.1002/ece3.7924

Bayer RJ, **Puttock CF**, **Kelchner SA. 2000**. Phylogeny of South African Gnaphalieae (Asteraceae) based on two noncoding chloroplast sequences. *American Journal of Botany* **87**: 259–272. doi:10.2307/2656914

Beentje HJ. 2002. Helichrysum. In: **Beentje HJ.** ed. *Flora of tropical East Africa; part 2*. Rotterdam: Balkema, 403–452.

Bergh NG, **Linder HP. 2009**. Cape diversification and repeated out-of-southern-Africa dispersal in paper daisies (Asteraceae-Gnaphalieae). *Molecular Phylogenetics and Evolution* **51**: 5–18. doi:10.1016/j.ympev.2008.09.001

Blanco-Gavaldà C, **Galbany-Casals M**, **Susanna A**, ***et al.* 2023**. Repeatedly northwards and upwards: southern African grasslands fuel the colonization of the African Sky Islands in *Helichrysum* (Compositae). *Plants* **12**: 2213. doi:10.3390/plants12112213

Blanco-Gavaldà C, **Roquet C**, **Puig-Surroca G**, ***et al.* 2025**. Biome conservatism prevailed in repeated long-distance colonization of Madagascar's mountains by *Helichrysum* (Compositae, Gnaphalieae). *Molecular Phylogenetics and Evolution* **204**: 108283. doi:10.1016/j.ympev.2024.108283

Blionis GJ, **Vokou D. 2001**. Pollination ecology of *Campanula* species on Mt Olympos, Greece. *Ecography* **24**: 287–297. doi:10.1034/j.1600-0587.2001.240306

Böhme M. 2003. The Miocene Climatic Optimum: evidence from ectothermic vertebrates of central Europe. *Palaeogeography, Palaeoclimatology, Palaeoecology* **195**: 389–401. doi:10.1016/S0031-0182(03)00367-5

Bolger AM, **Lohse M**, **Usadel B. 2014**. Trimmomatic: a flexible trimmer for Illumina sequence data. *Bioinformatics* **30**: 2114–2120. doi:10.1093/bioinformatics/btu170

Boucher FC, **Thuiller W**, **Roquet C**, ***et al.* 2012**. Reconstructing the origins of high-alpine niches and cushion life form in the genus *Androsace* S.L. (Primulaceae). *Evolution* **66**: 1255–1268. doi:10.1111/j.1558-5646.2011.01483.x

Bredenkamp G, **Spada F**, **Kazmierczak E. 2002**. On the origin of northern and southern hemisphere grasslands. *Plant Ecology* **163**: 209–229. doi:10.1023/A:1020957807971

Brochmann C, **Gizaw A**, **Chala D**, ***et al.* 2022**. History and evolution of the afroalpine flora: in the footsteps of Olov Hedberg. *Alpine Botany* **132**: 65–87. doi:10.1007/s00035-021-00256-9

Burnham KP, **Anderson DR. 1998**. *Model selection and inference: a practical information-theoretical approach*. New York: Springer.

Bushnell B. 2014. *BBMap: A Fast, Accurate, Splice-Aware Aligner*. www.ourceforge.net/projects/bbmap/

Carbutt C. 2019. The Drakensberg Mountain Centre: a necessary revision of Southern Africa's high-elevation centre of plant endemism. *South African Journal of Botany* **124**: 508–529. doi:10.1016/j.sajb.2019.05.032

Carbutt C, **Edwards TJ. 2004**. The flora of the Drakensberg Alpine Centre. *Edinburgh Journal of Botany* **60**: 581–607. doi:10.1017/S0960428603000428

Carnicero P, **Sáez L**, **Garcia-Jacas N**, **Galbany-Casals M. 2017**. Different speciation types meet in a Mediterranean genus: the biogeographic history of *Cymbalaria* (Plantaginaceae). *Taxon* **66**: 393–407. doi:10.12705/662.7

Carruthers T, **Moerland MS**, **Ebersbach J**, ***et al.* 2024**. Repeated upslope biome shifts in *Saxifraga* during late-Cenozoic climate cooling. *Nature Communications* **15**: 1100. doi:10.1038/s41467-024-45289-w

Chala D, **Zimmermann NE**, **Brochmann C**, **Bakkestuen V. 2017**. Migration corridors for alpine plants among the 'sky islands' of Eastern Africa: do they, or did they exist? *Alpine Botany* **127**: 133–144. doi:10.1007/s00035-017-0184-z

Chazot N, **Willmott KR**, **Condamine F**, ***et al.* 2016**. Into the Andes: multiple independent colonizations drive montane diversity in the Neotropical clearwing butterflies *Godyridina*. *Molecular Ecology* **25**: 5765–5784. doi:10.1111/mec.13773

Clark PU, **Archer D**, **Pollard D**, ***et al.* 2006**. The middle Pleistocene transition: characteristics, mechanisms, and implications for long-term changes in atmospheric pCO_2. *Quaternary Science Reviews* **25**: 3150–3184. doi:10.1016/j.quascirev.2006.07.008

Combrink LL, **Golcher-Benavides J**, **Lewanski AL**, **Rick JA**, **Rosenthal WC**, **Wagner CE. 2025**. Population genomics of adaptive radiation. *Molecular Ecology* **34**: e17574. doi:10.1111/mec.17574

Contreras-Ortiz N, **Atchison GW**, **Hughes CE**, **Madriñán S. 2018**. Convergent evolution of high elevation plant growth forms and geographically structured variation in Andean *Lupinus* (Fabaceae). *Botanical Journal of the Linnean Society* **187**: 118–136. doi:10.1093/botlinnean/box095

Costa FP, **Schrago CG**, **Mello B. 2022**. Assessing the relative performance of fast molecular dating methods for phylogenomic data. *BMC Genomics* **23**: 798. doi:10.1186/s12864-022-09030-5

Darriba D, **Posada D**, **Kozlov AM**, **Stamatakis A**, **Morel B**, **Flouri T. 2020**. ModelTest-NG: a new and scalable tool for the selection of DNA and protein evolutionary models. *Molecular Biology and Evolution* **37**: 291–294. doi:10.1093/molbev/msz189

Dellinger AS, **Lagomarsino L**, **Michelangeli F**, **Dullinger S**, **Smith SD. 2024**. The sequential direct and indirect effects of mountain uplift, climatic niche, and floral trait evolution on diversification dynamics in an Andean plant clade. *Systematic Biology* **73**: 594–612. doi:10.1093/sysbio/syae011

Dietrich L, **Körner C. 2014**. Thermal imaging reveals massive heat accumulation in flowers across a broad spectrum of alpine taxa. *Alpine Botany* **124**: 27–35. doi:10.1007/s00035-014-0123-1

Doebeli M, **Dieckmann U. 2003**. Speciation along environmental gradients. *Nature* **421**: 259–264. doi:10.1038/nature01274

Donoghue MJ. 2008. Colloquium paper: a phylogenetic perspective on the distribution of plant diversity. *Proceedings of the National Academy of Sciences of the United States of America* **105**: 11549–11555. doi:10.1073/pnas.0801962105

Donoghue MJ, **Edwards EJ. 2014**. Biome shifts and niche evolution in plants. *Annual Review of Ecology, Evolution, and Systematics* **45**: 547–572. doi:10.1146/annurev-ecolsys-120213-091905

Drummond CS. 2008. Diversification of *Lupinus* (Leguminosae) in the western new world: derived evolution of perennial life history and colonization of montane habitats. *Molecular Phylogenetics and Evolution* **48**: 408–421. doi:10.1016/j.ympev.2008.03.009

Drummond CS, **Eastwood RJ**, **Miotto STS**, **Hughes CE. 2012**. Multiple continental radiations and correlates of diversification in *Lupinus* (Leguminosae): testing for key innovation with incomplete taxon sampling. *Systematic Biology* **61**: 443–460. doi:10.1093/sysbio/syr126

Dupin J, **Matzke NJ**, **Särkinen T**, ***et al.* 2017**. Bayesian estimation of the global biogeographical history of the Solanaceae. *Journal of Biogeography* **44**: 887–899. doi:10.1111/jbi.12898

Dupont LM, **Rommerskirchen F**, **Mollenhauer G**, **Schefuß E. 2013**. Miocene to Pliocene changes in South African hydrology and vegetation in relation to the expansion of C4 plants. *Earth and Planetary Science Letters* **375**: 408–417. doi:10.1016/j.epsl.2013.06.005

Edwards EJ, **Donoghue MJ. 2013**. Is it easy to move and easy to evolve? Evolutionary accessibility and adaptation. *Journal of Experimental Botany* **64**: 4047–4052. doi:10.1093/jxb/ert220

Elias M, **Joron M**, **Willmott K**, ***et al.* 2009**. Out of the Andes: patterns of diversification in clearwing butterflies. *Molecular Ecology* **18**: 1716–1729. doi:10.1111/j.1365-294X.2009.04149.x

Etienne RS, **Haegeman B**, **Stadler T**, ***et al.* 2012**. Diversity-dependence brings molecular phylogenies closer to agreement with the fossil record. *Proceedings: Biological Sciences* **279**: 1300–1309. doi:10.1098/rspb.2011.1439

Felsenstein J. 1985. Confidence limits on phylogenies: an approach using the bootstrap. *Evolution* **39**: 783–791. doi:10.1111/j.1558-5646.1985.tb00420.x

Fér T, **Schmickl RE. 2018**. HybPhyloMaker: target enrichment data analysis from raw reads to species trees. *Evolutionary Bioinformatics Online* **14**: 1176934317742613. doi:10.1177/1176934317742613

FitzJohn RG. 2012. Diversitree: comparative phylogenetic analyses of diversification in R. *Methods in Ecology and Evolution* **3**: 1084–1092. doi:10.1111/j.2041-210X.2012.00234.x

Flantua SGA, **Hooghiemstra H. 2018**. Historical connectivity and mountain biodiversity. In: **Hoorn C**, **Perrigo A**, **Antonelli A.** eds. *Mountains, climate and biodiversity*, 1st edn. Oxford: Wiley-Blackwell, 171–185.

Flantua SGA, **O'Dea A**, **Onstein RE**, **Giraldo C**, **Hooghiemstra H. 2019**. The flickering connectivity system of the north Andean páramos. *Journal of Biogeography* **46**: 1808–1825. doi:10.1111/jbi.13607

Folk RA, **Charboneau JLM**, **Belitz M**, ***et al.* 2024**. Anatomy of a megaradiation: biogeography and niche evolution in *Astragalus*. *American Journal of Botany* **111**: e16299. doi:10.1002/ajb2.16299

Galbany-Casals M, **Garcia-Jacas N**, **Susanna A**, **Sáez L**, **Benedí C. 2004**. Phylogenetic relationships in the Mediterranean *Helichrysum* (Asteraceae, Gnaphalieae) based on nuclear rDNA ITS sequence data. *Australian Systematic Botany* **17**: 241–253. doi:10.1071/SB03031

Galbany-Casals M, **Romo AM. 2008**. Polyploidy and new chromosome counts in *Helichrysum* (Asteraceae, Gnaphalieae). *Botanical Journal of the Linnean Society* **158**: 511–521. doi:10.1111/j.1095-8339.2008.00889.x

Galbany-Casals M, **Unwin M**, **Garcia-Jacas N**, **Smissen RD**, **Susanna A**, **Bayer RJ. 2014**. Phylogenetic relationships in *Helichrysum* (Compositae: Gnaphalieae) and related genera: incongruence between nuclear and plastid phylogenies, biogeographic and morphological patterns, and implications for generic delimitation. *Taxon* **63**: 608–624. doi:10.12705/633.8

Galley C, **Linder HP. 2006**. Geographical affinities of the Cape flora, South Africa. *Journal of Biogeography* **33**: 236–250. doi:10.1111/j.1365-2699.2005.01376.x

Gamisch A, **Fischer GA**, **Comes HP. 2016**. Frequent but asymmetric niche shifts in *Bulbophyllum* orchids support environmental and climatic instability in Madagascar over Quaternary time scales. *BMC Evolutionary Biology* **16**: 14. doi:10.1186/s12862-016-0586-3

García MB, **Domingo D**, **Pizarro M**, **Font X**, **Gómez D**, **Ehrlén J. 2020**. Rocky habitats as microclimatic refuges for biodiversity. A close-up thermal approach. *Environmental and Experimental Botany* **170**: 103886. doi:10.1016/j.envexpbot.2019.103886

García-Moreno J, **Arctander P**, **Fjeldså J. 1998**. Pre-pleistocene differentiation among chat-tyrants. *The Condor: Ornithological Applications* **100**: 629–640. doi:10.2307/1369744

Gehrke B, **Kandziora M**, **Pirie MD. 2016**. The evolution of dwarf shrubs in alpine environments: a case study of *Alchemilla* in Africa. *Annals of Botany* **117**: 121–131. doi:10.1093/aob/mcv159

Gehrke B, **Linder HP. 2009**. The scramble for Africa: pan-temperate elements on the African high mountains. *Proceedings: Biological Sciences* **276**: 2657–2665. doi:10.1098/rspb.2009.0334

Gehrke B, **Linder HP. 2014**. Species richness, endemism and species composition in the tropical Afroalpine flora. *Alpine Botany* **124**: 165–177. doi:10.1007/s00035-014-0132-0

Godfree RC, **Marshall DJ**, **Young AG**, **Miller CH**, **Mathews S. 2017**. Empirical evidence of fixed and homeostatic patterns of polyploid advantage in a keystone grass exposed to drought and heat stress. *Royal Society Open Science* **4**: 170934. doi:10.1098/rsos.170934

Gorel A-P, **Hardy OJ**, **Dauby G**, ***et al.* 2022**. Climatic niche lability but growth form conservatism in the African woody flora. *Ecology Letters* **25**: 1164–1176. doi:10.1111/ele.13985

Gorospe JM, **Záveská E**, **Chala D**, ***et al.* 2025**. Ecological speciation with gene flow followed initial large-scale geographic speciation in the enigmatic afroalpine giant senecios (*Dendrosenecio*). *The New Phytologist* **246**: 2307–2323. doi:10.1111/nph.20432

Graae BJ, **Vandvik V**, **Armbruster WC**, ***et al.* 2018**. Stay or go—how topographic complexity influences alpine plant population and community responses to climate change. *Perspectives in Plant Ecology, Evolution and Systematics* **30**: 41–50. doi:10.1016/j.ppees.2017.09.008

Grytnes JA, **McCain CM. 2007**. Elevational trends in biodiversity. *Encyclopedia of Biodiversity* **2**: 1–8. doi:10.1016/B0122-2686(52)00503-4

Han T-S, **Hu Z-Y**, **Du Z-Q. 2022**. Adaptive responses drive the success of polyploid yellowcresses (*Rorippa*, Brassicaceae) in the Hengduan Mountains, a temperate biodiversity hotspot. *Plant Diversity* **44**: 455–467. doi:10.1016/j.pld.2022.02.002

Hedberg O. 1964. Features of afroalpine plant ecology. *Acta Phytogeographica Suecica* **49**: 1–144.

Hedberg I, **Hedberg O. 1979**. Tropical-alpine life forms of vascular plants. *Oikos* **33**: 297–307. doi:10.2307/3544006

Helmstetter AJ, **Zenil-Ferguson R**, **Sauquet H**, ***et al.* 2023**. Trait-dependent diversification in angiosperms: patterns, models and data. *Ecology Letters* **26**: 640–657. doi:10.1111/ele.14170

Herbert T, **Lawrence K**, **Tzanova A**, **Cleaveland Peterson L**, **Caballero-Gill R**, **Kelly CS. 2016**. Late Miocene global cooling and the rise of modern ecosystems. *Nature Geoscience* **9**: 843–847. doi:10.1038/ngeo2813

Herrando-Moraira S, **Roquet C**, **Calleja JA**, ***et al.* 2023**. Impact of the climatic changes in the Pliocene-Pleistocene transition on Irano-Turanian species. The radiation of genus *Jurinea* (Compositae). *Molecular Phylogenetics and Evolution* **189**: 107928. doi:10.1016/j.ympev.2023.107928

Herrera-Alsina L, **van Els P**, **Etienne RS. 2019**. Detecting the dependence of diversification on multiple traits from phylogenetic trees and trait data. *Systematic Biology* **68**: 317–328. doi:10.1093/sysbio/syy057

Hilliard OM. 1983. *Helichrysum* Mill. In: **Leistner OA.** ed. *Flora of Southern Africa; volume 33, part 7, fascicle 2*. Pretoria: Department of Agriculture, 61–310.

Hillis DM, **Bull JJ. 1993**. An empirical test of bootstrapping as a method for assessing confidence in phylogenetic analyses. *Systematic Biology* **42**: 182–192. doi:10.1093/sysbio/42.2.182

Hooft van Huysduynen A, **Janssens S**, **Merckx V**, ***et al.* 2021**. Temporal and paleoclimatic context of the evolution of insular woodiness in the Canary Islands. *Ecology and Evolution* **11**: 12220–12231. doi:10.1002/ece3.7986

Hughes CE, **Atchison GW. 2015**. The ubiquity of alpine plant radiations: from the Andes to the Hengduan Mountains. *The New Phytologist* **207**: 275–282. doi:10.1111/nph.13230

Hughes C, **Eastwood R. 2006**. Island radiation on a continental scale: exceptional rates of plant diversification after uplift of the Andes. *Proceedings of the National Academy of Sciences of the United States of America* **103**: 10334–10339. doi:10.1073/pnas.0601928103

Humbert H. 1962. Composées, part 2,189e famille. In: **Leroy JF.** ed. *Flore de Madagascar et des Comores (Plantes vasculaires)*. Paris: Muséum National d'Histoire Naturelle, 389–565.

Jabbour F, **Renner SS. 2012**. A phylogeny of Delphinieae (Ranunculaceae) shows that *Aconitum* is nested within *Delphinium* and that Late Miocene transitions to long life cycles in the Himalayas and Southwest China coincide with bursts in diversification. *Molecular Phylogenetics and Evolution* **62**: 928–942. doi:10.1016/j.ympev.2011.12.005

Jones MM, **Szyska B**, **Kessler M. 2011**. Microhabitat partitioning promotes plant diversity in a tropical montane forest. *Global Ecology and Biogeography* **20**: 558–569. doi:10.1111/j.1466-8238.2010.00627.x

Junier T, **Zdobnov EM. 2010**. The Newick utilities: high-throughput phylogenetic tree processing in the UNIX shell. *Bioinformatics* **26**: 1669–1670. doi:10.1093/bioinformatics/btq243

Kandziora M, **Gehrke B**, **Popp M**, **Gizaw A**, **Brochmann C**, **Pirie MD. 2022**. The enigmatic tropical alpine flora on the African sky islands is young, disturbed, and unsaturated. *Proceedings of the National Academy of Sciences of the United States of America* **119**: e2112737119. doi:10.1073/pnas.2112737119

Kandziora M, **Kadereit JW**, **Gehrke B. 2016**. Frequent colonization and little in situ speciation in *Senecio* in the tropical alpine-like islands of Eastern Africa. *American Journal of Botany* **103**: 1483–1498. doi:10.3732/ajb.1600210

Katoh K, **Toh H. 2008**. Recent developments in the MAFFT multiple sequence alignment program. *Briefings in Bioinformatics* **9**: 286–298. doi:10.1093/bib/bbn013

Kebede M, **Ehrich D**, **Taberlet P**, **Nemomissa S**, **Brochmann C. 2007**. Phylogeography and conservation genetics of a giant lobelia (*Lobelia giberroa*) in Ethiopian and Tropical East African mountains. *Molecular Ecology* **16**: 1233–1243. doi:10.1111/j.1365-294X.2007.03232.x

Knox EB, **Palmer JD. 1995**. Chloroplast DNA variation and the recent radiation of the giant senecios (Asteraceae) on the tall mountains of Eastern Africa. *Proceedings of the National Academy of Sciences of the United States of America* **92**: 10349–10353. doi:10.1073/pnas.92.22.10349

Körner C. 2021. *Alpine plant life: functional plant ecology of high mountain ecosystems*. Cham: Springer.

Körner C, **Paulsen J**, **Spehn EM. 2011**. A definition of mountains and their bioclimatic belts for global comparisons of biodiversity data. *Alpine Botany* **121**: 73–78. doi:10.1007/s00035-011-0094-4

Kozlov AM, **Darriba D**, **Flouri T**, **Morel B**, **Stamatakis A. 2019**. RAxML-NG: a fast, scalable, and user-friendly tool for maximum likelihood phylogenetic inference. *Bioinformatics* **35**: 4453–4455. doi:10.1093/bioinformatics/btz305

Kumar S, **Stecher G**, **Li M**, **Knyaz C**, **Tamura K. 2018**. MEGA X: molecular evolutionary genetics analysis across computing platforms. *Molecular Biology and Evolution* **35**: 1547–1549. doi:10.1093/molbev/msy096

Landis MJ, **Matzke NJ**, **Moore BR**, **Huelsenbeck JP. 2013**. Bayesian analysis of biogeography when the number of areas is large. *Systematic Biology* **62**: 789–804. doi:10.10933/sysbio/syt040

Lefebvre V, **Villemant C**, **Fontaine C**, **Daugeron C. 2018**. Altitudinal, temporal and trophic partitioning of flower-visitors in Alpine communities. *Scientific Reports* **8**: 4706. doi:10.1038/s41598-018-23210-y

Lemoine F, **Domelevo Entfellner JB**, **Wilkinson E**, ***et al.*** **2018**. Renewing Felsenstein's phylogenetic bootstrap in the era of big data. *Nature* **556**: 452–456. doi:10.1038/s41586-018-0043-0

Li H, **Durbin R. 2009**. Fast and accurate short-read alignment with Burrows-Wheeler transform. *Bioinformatics* **25**: 1754–1760. doi:10.1093/bioinformatics/btp324

Linder HP. 2003. The radiation of the Cape flora, Southern Africa. *Biological Reviews* **78**: 597–638. doi:10.1017/S1464793103006171

Linder HP. 2014. The evolution of African plant diversity. *Frontier in Ecology and Evolution* **2**: 38. doi:10.3389/fevo.2014.00038

Linder HP, **Hardy CR**, **Rutschmann F. 2005**. Taxon sampling effects in molecular clock dating: an example from the African Restionaceae. *Molecular Phylogenetics and Evolution* **35**: 569–582. doi:10.1016/j.ympev.2004.12.006

Linder HP, **Verboom GA. 2015**. The evolution of regional species richness: the history of the Southern African flora. *Annual Review of Ecology, Evolution, and Systematics* **46**: 393–412. doi:10.1146/annurev-ecolsys-112414-054322

Lisowski S. 1989. *Helichrysum* Compositae (deuxième partie: tribu Inuleae). In: **Lisowski S.** ed. *Flore d'Afrique Centrale (Zaïre, Rwanda, Burundi)*. Meise: National Botanic Garden of Belgium, 68–192.

Liu K, **Li E**, **Cui X**, ***et al.*** **2024**. Key innovations and niche variation promoted rapid diversification of the widespread Juniperus (Cupressaceae). *Communications Biology* **7**: 1002. doi:10.1038/s42003-024-06687-4

Louca S, **Pennell MW. 2020**. Extant time trees are consistent with a myriad of diversification histories. *Nature* **580**: 502–505. doi:10.1038/s41586-020-2176-1

Louca S, **Pennell MW. 2021**. Why extinction estimates from extant phylogenies are so often zero. *Current Biology: CB* **31**: 3168–3173.e4. doi:10.1016/j.cub.2021.04.066

Luebert F, **Weigend M. 2014**. Phylogenetic insights into Andean plant diversification. *Frontiers in Ecology and Evolution* **2**: 27. doi:10.3389/fevo.2014.00027

Madriñán S, **Cortés AJ**, **Richardson JE. 2013**. Páramo is the world's fastest evolving and coolest biodiversity hotspot. *Frontiers in Genetics* **4**: 192. doi:10.3389/fgene.2013.00192

Mandel JR, **Dikow RB**, **Funk VA**, ***et al.*** **2014**. A target enrichment method for gathering phylogenetic information from hundreds of loci: an example from the Compositae. *Applications in Plant Sciences* **2**: apps.1300085. doi:10.3732/apps.1300085

Mandel JR, **Dikow RB**, **Siniscalchi CM**, **Thapa R**, **Watson LE**, **Funk VA. 2019**. A fully resolved backbone phylogeny reveals numerous dispersals and explosive diversifications throughout the history of Asteraceae. *Proceedings of the National Academy of Sciences of the United States of America* **116**: 14083–14088. doi:10.1073/pnas.1903871116

Marchant DB, **Soltis DE**, **Soltis PS. 2016**. Patterns of abiotic niche shifts in allopolyploids relative to their progenitors. *The New Phytologist* **212**: 708–718. doi:10.1111/nph.14069

Martín-Hernanz S, **Albaladejo RG**, **Lavergne S. 2023**. Strong conservatism of floral morphology during the rapid diversification of the genus *Helianthemum*. *American Journal of Botany* **110**: e16155. doi:10.1002/ajb2.16155

Matzke NJ. 2013. Probabilistic historical biogeography: new models for founder-event speciation, imperfect detection, and fossils allow improved accuracy and model-testing. *Frontiers of Biogeography* **5**: 242–248. doi:10.21425/F55419694

Matzke NJ. 2022. Statistical comparison of DEC and DEC+J is identical to comparison of two ClaSSE submodels, and is therefore valid. *Journal of Biogeography* **49**: 1805–1824. doi:10.1111/jbi.14346

Merckx VS, **Hendriks KP**, **Beentjes KK**, ***et al.*** **2015**. Evolution of endemism on a young tropical mountain. *Nature* **524**: 347–350. doi:10.1038/nature14949

Meudt HM, **Albach DC**, **Tanentzap AJ. 2021**. Polyploidy on islands: its emergence and importance for diversification. *Frontiers in Plant Science* **12**: 637214. doi:10.3389/fpls.2021.637214

Meudt HM, **Pearson SM**, **Ning W**, **Prebble JM**, **Tate JA. 2025**. Forget-me-not phylogenomics: improving the resolution and taxonomy of a rapid island and mountain radiation in Aotearoa New Zealand (*Myosotis*; Boraginaceae). *Molecular Phylogenetics and Evolution* **204**: 108250. doi:10.1016/j.ympev.2024.108250

Miller AH, **Stroud JT**, **Losos JB. 2023**. The ecology and evolution of key innovations. *Trends in Ecology & Evolution* **38**: 122–131. doi:10.1016/j.tree.2022.09.005

Minorsky PV. 2019. The functions of foliar nyctinasty: a review and hypothesis. *Biological Reviews* **94**: 216–229. doi:10.1111/brv.12444

Monasterio M, **Sarmiento L. 1991**. Adaptive radiation of *Espeletia* in the cold Andean tropics. *Trends in Ecology and Evolution* **6**: 387–391. doi:10.1016/0169-5347(91)90159-U

Montes-Moreno N, **Sáez L**, **Benedí C**, **Susanna A**, **Garcia-Jacas N. 2010**. Generic delineation, phylogeny and subtribal affinities of *Phagnalon* and *Aliella* (Compositae, Gnaphalieae) based on nuclear and chloroplast sequences. *Taxon* **59**: 1654–1670. doi:10.1002/tax.596002

Morales-Briones DF, **Liston A**, **Tank DC. 2018**. Phylogenomic analyses reveal a deep history of hybridization and polyploidy in the Neotropical genus *Lachemilla* (Rosaceae). *The New Phytologist* **218**: 1668–1684. doi:10.1111/nph.15099

Morlon H, **Lewitus E**, **Condamine FL**, **Manceau M**, **Clavel J**, **Drury JP. 2016**. RPANDA: an R package for macroevolutionary analyses on phylogenetic trees. *Methods in Ecology and Evolution* **7**: 589–597. doi:10.1111/2041-210X.12526

Morlon H, **Robin S**, **Hartig F. 2022**. Studying speciation and extinction dynamics from phylogenies: addressing identifiability issues. *Trends in Ecology & Evolution* **37**: 497–506. doi:10.1016/j.tree.2022.02.004

Muellner-Riehl AN, **Schnitzler J**, **Kissling WD**, ***et al.*** **2019**. Origins of global mountain plant biodiversity: testing the 'mountain-geobiodiversity hypothesis'. *Journal of Biogeography* **46**: 2826–2838. doi:10.1111/jbi.13715

Mynard P, **Algar AC**, **Lancaster LT**, ***et al.*** **2023**. Impact of phylogenetic tree completeness and mis-specification of sampling fractions on trait dependent diversification models. *Systematic Biology* **72**: 106–119. doi:10.1093/sysbio/syad001

Neumann FH, **Bamford MK. 2015**. Shaping of modern Southern African biomes: Neogene vegetation and climate changes. *Transactions of the Royal Society of South Africa* **70**: 195–212. doi:10.1080/0035919X.2015.1072859

Nie Z-L, **Funk VA**, **Meng Y**, **Deng T**, **Sun H**, **Wen J. 2016**. Recent assembly of the global herbaceous flora: evidence from the paper daisies (Asteraceae: Gnaphalieae). *The New Phytologist* **209**: 1795–1806. doi:10.1111/nph.13740

Novikova PY, **Hohmann N**, **Van de Peer Y. 2018**. Polyploid *Arabidopsis* species originated around recent glaciation maxima. *Current Opinion in Plant Biology* **42**: 8–15. doi:10.1016/j.pbi.2018.01.005

Nürk NM, **Atchison GW**, **Hughes CE. 2019**. Island woodiness underpins accelerated disparification in plant radiations. *The New Phytologist* **224**: 518–531. doi:10.1111/nph.15797

Nürk NM, **Linder HP**, **Onstein RE**, ***et al.* 2020**. Diversification in evolutionary arenas—assessment and synthesis. *Ecology and Evolution* **10**: 6163–6182. doi:10.1002/ece3.6313

Nürk NM, **Michling F**, **Linder HP. 2018**. Are the radiations of temperate lineages in tropical alpine ecosystems pre-adapted? *Global Ecology and Biogeography* **27**: 334–345. doi:10.1111/geb.12699

Nürk NM, **Uribe-Convers S**, **Gehrke B**, **Tank DC**, **Blattner FR. 2015**. Oligocene niche shift, Miocene diversification—cold tolerance and accelerated speciation rates in the St. John's worts (*Hypericum*, Hypericaceae). *BMC Ecology and Evolution* **15**: 80. doi:10.1186/s12862-015-0359-4

Onstein RE. 2020. Darwin's second 'abominable mystery': trait flexibility as the innovation leading to angiosperm diversity. *The New Phytologist* **228**: 1741–1747. doi:10.1111/nph.16294

Pachschwöll C, **Escobar García P**, **Winkler M**, **Schneeweiss GM**, **Schönswetter P. 2015**. Polyploidisation and geographic differentiation drive diversification in a European high mountain plant group (*Doronicum clusii* Aggregate, Asteraceae). *PLoS One* **10**: e0118197. doi:10.1371/journal.pone.0118197

Pagel M, **Meade A**, **Barker D. 2004**. Bayesian estimation of ancestral character states on phylogenies. *Systematic Biology* **53**: 673–684. doi:10.1080/10635150490522232

Partridge TC. 1998. Of diamonds, dinosaurs and diastrophism: 150 years of landscape evolution in Southern Africa. *South African Geographical Journal* **101**: 167–184.

Partridge TC, **Maud RR. 2000**. Macro-scale geomorphic evolution of Southern Africa. In: **Partridge TC**, **Maud RR.** eds. *The Cenozoic of Southern Africa*. Oxford: Oxford University Press, 3–18.

Pérez-Escobar OA, **Zizka A**, **Bermúdez MA**, ***et al.* 2022**. The Andes through time: evolution and distribution of Andean floras. *Trends in Plant Science* **27**: 364–378. doi:10.1016/j.tplants.2021.09.010

Perrigo A, **Hoorn C**, **Antonelli A. 2020**. Why mountains matter for biodiversity. *Journal of Biogeography* **47**: 315–325. doi:10.1111/jbi.13731

Pirie MD, **Kandziora M**, **Nürk NM**, ***et al.* 2019**. Leaps and bounds: geographical and ecological distance constrained the colonisation of the Afrotemperate by Erica. *BMC Evol Biol* **19**: 222. doi:10.1186/s12862-019-1545-6

Rabosky DL. 2010. Extinction rates should not be estimated from molecular phylogenies. *Evolution; International Journal of Organic Evolution* **64**: 1816–1824. doi:10.1111/j.1558-5646.2009.00926.x

Rahbek C, **Borregaard MK**, **Antonelli A**, ***et al.* 2019**. Building mountain biodiversity: geological and evolutionary processes. *Science* **365**: 1114–1119. doi:10.1126/science.aax0151

Ramalho RS, **Brum da Silveira A**, **Fonseca PE. 2015**. The emergence of volcanic oceanic islands on a slow-moving plate: the example of Madeira Island, NE Atlantic. *Geochemistry, Geophysics, Geosystems: G(3)* **16**: 522–537. doi:10.1002/2014GC005657

Ramsey J. 2011. Polyploidy and ecological adaptation in wild yarrow. *Proceedings of the National Academy of Sciences of the United States of America* **108**: 7096–7101. doi:10.1073/pnas.1016631108

Ree RH, **Moore BR**, **Webb CO**, **Donoghue MJ. 2005**. A likelihood framework for inferring the evolution of geographic range on phylogenetic trees. *Evolution; International Journal of Organic Evolution* **45**: 2299–2311. doi:10.1111/j.0014-3820.2005.tb00940.x

Ree RH, **Sanmartín I. 2018**. Conceptual and statistical problems with the DEC +J model of founder-event speciation and its comparison with DEC via model selection. *Journal of Biogeography* **45**: 741–749. doi:10.1111/jbi.13173

Ree RH, **Smith SA. 2008**. Maximum likelihood inference of geographic range evolution by dispersal, local extinction and cladogenesis. *Systematic Biology* **57**: 4–14. doi:10.1080/10635150701883881

Rice A, **Šmarda P**, **Novosolov M**, ***et al.* 2019**. The global biogeography of polyploid plants. *Nature Ecology and Evolution* **3**: 265–273. doi:10.1038/s41559-018-0787-9

Roberts D, **Cawthra H**, **Musekiwa C. 2014**. Dynamics of late Cenozoic aeolian deposition along the South African coast: a record of evolving climate and ecosystems. *Geological Society* **388**: 353–387. doi:10.1144/SP388.11

Ronquist F. 1997. Dispersal-vicariance analysis: a new approach to the quantification of historical biogeography. *Systematic Biology* **46**: 195–203. doi:10.2307/2413643

Roquet C, **Boucher FC**, **Thuiller W**, **Lavergne S. 2013**. Replicated radiations of the alpine genus *Androsace* (Primulaceae) driven by range expansion and convergent key innovations. *Journal of Biogeography* **40**: 1874–1886. doi:10.1111/jbi.12135

Roy MS. 1997. Recent diversification in African greenbuls (Pycnonotidae: Andropadus) supports a montane speciation model. *Proc Biol Sci.* **264**: 1337–1344. doi:10.1098/rspb.1997.0185

Rudbeck AV, **Sun M**, **Tietje M**, ***et al.* 2022**. The Darwinian shortfall in plants: phylogenetic knowledge is driven by range size. *Ecography* **2022**: e06142. doi:10.1111/ecog.06142

Rull V. 2005. Biotic diversification in the Guayana Highlands: a proposal. *Journal of Biogeography* **32**: 921–927. doi:10.1111/j.1365-2699.2005.01252.x

Rundell RJ, **Price TD. 2009**. Adaptive radiation, nonadaptive radiation, ecological speciation and nonecological speciation. *Trends in Ecology and Evolution* **24**: 394–399. doi:10.1016/j.tree.2009.02.007

Sandel B, **Monnet AC**, **Govaerts R**, **Vorontsova M. 2017**. Late Quaternary climate stability and the origins and future of global grass endemism. *Annals of Botany* **119**: 279–288. doi:10.1093/aob/mcw178

Sayyari E, **Mirarab S. 2016**. Fast coalescent-based computation of local branch support from quartet frequencies. *Molecular Biology and Evolution* **33**: 1654–1668. doi:10.1093/molbev/msw079

Schmidt-Lebuhn AN, **Bovill J. 2021**. Phylogenomic data reveal four major clades of Australian Gnaphalieae (Asteraceae). *Taxon* **70**: 1020–1034. doi:10.1002/tax.12510

Schwartz RS, **Mueller RL. 2010**. Branch length estimation and divergence dating: estimates of error in Bayesian and maximum likelihood frameworks. *BMC Evolutionary Biology* **10**: 5. doi:10.1186/1471-2148-10-5

Schwery O, **Onstein RE**, **Bouchenak-Khelladi Y**, **Xing Y**, **Carter RJ**, **Linder HP. 2015**. As old as the mountains: the radiations of the Ericaceae. *The New Phytologist* **207**: 355–367. doi:10.1111/nph.13234

Sedano RE, **Burns KJ. 2010**. Are the Northern Andes a species pump for Neotropical birds? Phylogenetics and biogeography of a clade of Neotropical tanagers (Aves: Thraupini). *Journal of Biogeography* **37**: 325–343. doi:10.1111/j.1365-2699.2009.02200.x

Sepulchre P, **Ramstein G**, **Fluteau F**, **Schuster M**, **Tercelin JJ**, **Brunet M. 2006**. Tectonic uplift and Eastern Africa aridification. *Science* **313**: 1419–1423. doi:10.10520/EJC-947b4efa3

Skeels A. 2019. Lineages through space and time plots: visualising spatial and temporal changes in diversity. *Frontiers of Biogeography* **11**: e42954. doi:10.21425/F5FBG42954

Sklenář P, **Dušková E**, **Balslev H. 2011**. Tropical and temperate: evolutionary history of Páramo flora. *Botanical Reviews* **77**: 71–108. doi:10.1007/s12229-010-9061-9

Slovák M, **Melichárková A**, **Štubňová EG**, ***et al.* 2023**. Pervasive introgression during rapid diversification of the European mountain genus *Soldanella* (L.) (Primulaceae). *Systematic Biology* **72**: 491–504. doi:10.1093/sysbio/syac071

Smissen RD, **Bayer RJ**, **Bergh NG**, ***et al.* 2020**. A revised subtribal classification of Gnaphalieae (Asteraceae). *Taxon* **69**: 778–806. doi:10.1002/tax.12294

Smissen RD, **Galbany-Casals M**, **Breitwieser I. 2011**. Ancient allopolyploidy in the everlasting daisies (Asteraceae: Gnaphalieae): complex relationships among extant clades. *Taxon* **60**: 649–662. doi:10.1002/tax.603003

Smyčka J, **Roquet C**, **Boleda M**, ***et al.* 2022**. Tempo and drivers of plant diversification in the European mountain system. *Nature Communications* **13**: 2750. doi:10.1038/s41467-022-30394-5

Stamatakis A. 2014. RAxML version 8: a tool for phylogenetic analysis and post-analysis of large phylogenies. *Bioinformatics* **30**: 1312–1313. doi:10.1093/bioinformatics/btu033

Tadesse M. 2004. *Helichrysum* Mill., Asteraceae (Compositae). In: **Hedberg I**, **Friis I**, **Edwards S.** eds. *Flora of Ethiopia and Eritrea; part 2*. Addis Ababa: Addis Abeba University, 163–178.

Tamura K, **Battistuzzi FU**, **Billing-Ross P**, **Murillo O**, **Filipski A**, **Kumar S. 2012**. Estimating divergence times in large molecular phylogenies. *Proceedings of the National Academy of Sciences of the United States of America* **109**: 19333–19338. doi:10.1073/pnas.1213199109

Tamura K, **Tao Q**, **Kumar S. 2018**. Theoretical foundation of the RelTime methods for estimating divergence times from variable evolutionary rates. *Molecular Biology and Evolution* **35**: 1770–1782. doi:10.1093/molbev/msy044

Tao Q, **Tamura K**, **Mello B**, **Kumar S. 2020**. Reliable confidence intervals for RelTime estimates of evolutionary divergence times. *Molecular Biology and Evolution* **37**: 280–290. doi:10.1093/molbev/msz236

Tenorio EA, **Montoya P**, **Norden N**, **Rodríguez-Buriticá S**, **Salgado-Negret B**, **Gonzalez MA. 2023**. Mountains exhibit a stronger latitudinal diversity gradient than lowland regions. *Journal of Biogeography* **50**: 1026–1036. doi:10.1111/jbi.14597

Thomas A, **Meudt HM**, **Larcombe MJ**, ***et al.* 2023**. Multiple origins of mountain biodiversity in New Zealand's largest plant radiation. *Journal of Biogeography* **50**: 947–960. doi:10.1111/jbi.14589

Tietje M, **Antonelli A**, **Baker WJ**, **Govaerts R**, **Smith SA**, **Eiserhardt WL. 2022**. Global variation in diversification rate and species richness are unlinked in plants. *Proceedings of the National Academy of Sciences of the United States of America* **119**: e2120662119. doi:10.1073/pnas.2120662119

Ufimov R, **Gorospe JM**, **Fér T**, ***et al.* 2022**. Utilizing paralogues for phylogenetic reconstruction has the potential to increase species tree support and reduce gene tree discordance in target enrichment data. *Molecular Ecology Resources* **22**: 3018–3034. doi:10.1111/1755-0998.13684

Van de Peer Y, **Ashman TL**, **Soltis PS**, **Soltis DE. 2021**. Polyploidy: an evolutionary and ecological force in stressful times. *The Plant Cell* **33**: 11–26. doi:10.1093/plcell/koaa015

Van de Peer Y, **Mizrachi E**, **Marchal K. 2017**. The evolutionary significance of polyploidy. *Nature Reviews: Genetics* **18**: 411–424. doi:10.1038/nrg.2017.26

Van Els P, **Herrera-Alsina L**, **Pigot AL**, **Etienne RS. 2021**. Evolutionary dynamics of the elevational diversity gradient in passerine birds. *Nature Ecology & Evolution* **5**: 1259–1265. doi:10.1038/s41559-021-01515-y

Wen J, **Zhang JQ**, **Nie ZL**, **Zhong Y**, **Sun H. 2014**. Evolutionary diversifications of plants on the Qinghai-Tibetan Plateau. *Frontiers in Genetics* **5**: 4. doi:10.3389/fgene.2014.00004

Westerhold T, **Marwan N**, **Dryry AJ**, ***et al.* 2020**. An astronomically dated record of Earth's climate and its predictability over the last 66 million years. *Science* **369**: 1383–1387. doi:10.1126/science.aba6853

Wiens JJ, **Ackerly DD**, **Allen AP**, ***et al.* 2010**. Niche conservatism as an emerging principle in ecology and conservation biology. *Ecology Letters* **13**: 1310–1324. doi:10.1111/j.1461-0248.2010.01515.x

Wiens JJ, **Graham CH. 2005**. Niche conservatism: integrating evolution, ecology, and conservation biology. *Annual Review of Ecology, Evolution, and Systematics* **36**: 519–539. doi:10.1146/annurev.ecolsys.36.102803.095431

Winkler M, **Lamprecht A**, **Steinbauer K**, ***et al.* 2016**. The rich sides of mountain summits—a pan-European view on aspect preferences of alpine plants. *Journal of Biogeography* **43**: 2261–2273. doi:10.1111/jbi.12835

Ye X-Y, **Ma P-F**, **Yang G-Q**, ***et al.* 2019**. Rapid diversification of alpine bamboos associated with the uplift of the Hengduan Mountains. *Journal of Biogeography* **46**: 2678–2689. doi:10.1111/jbi.13723

Yu H, **Miao S**, **Xie G**, **Guo X**, **Chen Z**, **Favre A. 2020**. Contrasting floristic diversity of the Hengduan Mountains, the Himalayas and the Qinghai-Tibet Plateau sensu stricto in China. *Frontiers in Ecology and Evolution* **8**: 136. doi:10.3389/fevo.2020.00136

Zachos J, **Dickens G**, **Zeebe R. 2008**. An early Cenozoic perspective on greenhouse warming and carbon-cycle dynamics. *Nature* **451**: 279–283. doi:10.1038/nature06588

Zachos J, **Pagani M**, **Sloan L**, ***et al.* 2001**. Trends, rhythms, and aberrations in global climate 65 Ma to present. *Science* **292**: 686–693. doi:10.1126/science.1059412

Zhang C, **Rabiee M**, **Sayyari E**, **Mirarab S. 2018**. ASTRAL-III: polynomial time species tree reconstruction from partially resolved gene trees. *BMC Bioinformatics* **19**: 153. doi:10.1186/s12859-018-2129-y

Zizka A, **Onstein RE**, **Rozzi R**, ***et al.* 2022**. The evolution of insular woodiness. *Proceedings of the National Academy of Sciences of the United States of America* **119**: e2208629119. doi:10.1073/pnas.2208629119